Nonlinear magnetoacoustic waves in plasma with isentropic thermal instability

D. I. Zavershinskii ⬡,* N. E. Molevich ⬡, D. S. Riashchikov ⬡, and S. A. Belov ⬡
Department of Physics, Samara National Research University, Moscovskoe sh. 34, Samara, 443086, Russia
and Department of Theoretical Physics, Lebedev Physical Institute, Novo-Sadovaya st. 221, Samara, 443011, Russia

Evolution of magnetoacoustic (MA) waves in the heat-releasing plasma is analyzed. Due to the temperature and density dependence of the heating and cooling processes, the dispersion properties of MA waves in the considered medium is rather specific. The dispersion of phase velocity can be either positive or negative, and waves can be further damped or amplified. The amplification of MA waves takes place in the case of isentropic instability. In order to analyze waves in such a medium, we use an approach based on an analogy between nonequilibrium relaxing gas and heat-releasing plasma. The uncompensated isentropic instability restricts the applicability of linear equations describing evolution of magnetoacoustic waves. It appears that for a stabilization of the isentropic instability to be reached, the inclusion of quadratic nonlinear terms is sufficient. In the current research, we derive the nonlinear magnetoacoustic equation (NMAE), which can describe evolution of fast and slow MA waves. The obtained nonlinear equation is different from the known analogues used for the analysis of waves in the considered type of medium, which are modifications of Korteweg–de Vries or Burgers equations. In contrast to the known analogues, it is obtained without the restrictions on wave spectrum and takes into account the main features of nonadiabatic processes that affect the formation of stationary wave structures. We describe analytical solutions of this equation in the form of shock waves including the self-sustained (autowave) pulse and investigate the dependence of these waves on the direction and magnitude of the external magnetic field. The evolutionary stability of the obtained structures is confirmed with the help of numerical solutions of the NMAE. The applicability of NMAE and the correctness of its solutions have been confirmed by the numerical solution of the initial system of magnetohydrodinamic equations. It is shown that the self-sustained (autowave) pulses, which may be realized only in the case of isentropic instability, completely recover their shape after the collision.

I. INTRODUCTION

A weak localized gasdynamic perturbation is able to generate periodic or quasiperiodic wave trains in a dispersive medium due to frequency dependence of phase velocity. Generally, amplitudes of waves in this case will decrease in the course of propagation due to the geometric factor or some dissipative processes in the medium and the perturbation will tend to disappear. A simple example is the diverging circles seen on the water as a result of a stone thrown into it.

However, the situation becomes much more intriguing if the dispersive medium is capable to amplify gasdynamic disturbances and wave increment depends on frequency as well as phase velocity does. As shown in Refs. [1–3], such conditions may take place in the so-called nonequilibrium media, where the nonequilibrium state of internal degrees of freedom is stationary maintained. For example, in the relaxing gas the vibrational energy of molecules in the discharge plasma can exceed its equilibrium value corresponding to the translational temperature of the medium. The specific combination of dispersion and amplification significantly affects both linear and nonlinear stages of the perturbation evolution. Particularly, it has been shown that in the nonlinear regime a localized perturbation of stationary state of the medium tends to generate a sequence of so-called autowave shock pulses [1,4]. Hereinafter, the term "autowaves" corresponds to the self-sustaining waves, which shape and amplitude depend only on the properties of the medium. It has been shown in Refs. [1,5,6] that the profile of autowave pulses in such a medium can be analytically described by using the solution of generalized nonlinear acoustic equation (NAE), which has been obtained without restriction on the spectrum of acoustic waves and, therefore, can adequately describe stationary wave structures.

Another example of the dispersive medium, where phase velocity and wave increment/decrement are both frequency dependent, is the heat-releasing medium. Rayleigh, in his study of the sound vibrations maintained by heat (e.g., singing flames), formulated a criterion for the amplification of sound: "If heat given to the air at the moment of greatest condensation, or be taken from it at the moment of greatest rarefaction, the vibration is encouraged. On other hand, if heat be given at the moment or greatest rarefaction, or abstracted at the moment of greatest condensation, the vibration is discouraged" (see Ref. [7], p. 226).

In order to describe the processes in the heat-releasing media, Field in his pioneer paper [8] introduced in the heat transfer equation the so-called generalized heat-loss function:

$$Q(\rho, T) = L(\rho, T) - H(\rho, T). \tag{1}$$

This function is defined as the difference between power of the radiative energy losses $L(\rho, T)$ and the power of the

*dimanzav@mail.ru

energy gain $H(\rho, T)$ without taking into account the thermal conductivity. Here, ρ, T are the local density and temperature of the medium, respectively. For a stationary state of the medium, heating and cooling powers are balanced, and the generalized heat-loss function is assumed to be zero:

$$Q(\rho_0, T_0) = 0. \tag{2}$$

It should be noted that function (1) can be written as a function of local values of ρ and T, if the gas is sufficiently diffuse to be considered optically thin, since under this conditions the interaction between gas and some radiation field is not complicated by radiative transfer effects [8,9]. This approach is fully applicable to such rarefied media like the interstellar gas and solar atmosphere.

By using this function Q in the heat transfer equation, it was shown that three kinds of instability can be realized in the heat-releasing medium [8]: isochoric, isobaric, and isentropic.

The criterion of isochoric thermal instability (first proposed by Parker [10]) corresponds to

$$\left(\frac{\partial Q}{\partial T}\right)_\rho < 0. \tag{3}$$

However, the pressure variations accompanying isochoric changes in temperature are to excite the motions of the medium which, as a result, will destroy constancy of density [8].

The criterion of isobaric thermal instability corresponds to

$$\left(\frac{\partial Q}{\partial T}\right)_\rho - \frac{\rho_0}{T_0}\left(\frac{\partial Q}{\partial \rho}\right)_T < 0. \tag{4}$$

The analysis of this thermal instability mode (the so-called condensation or entropy mode) makes it possible, in particular, to explain the observations of the interstellar gas separation into two phases: cold dense clouds and diffuse warm intercloud medium in pressure equilibrium (see, for example, Refs. [11–14]).

In the present paper, these two types of thermal instability are not considered, though. The main attention is paid to nonlinear structures formed under the condition of the third type of thermal instability, namely, the isentropic (acoustic) instability. According to Ref. [8], the isentropic instability criterion has the following form:

$$\left(\frac{\partial Q}{\partial T}\right)_\rho + \frac{\rho_0}{T_0(\gamma - 1)}\left(\frac{\partial Q}{\partial \rho}\right)_T < 0. \tag{5}$$

In this case, a positive feedback is established between the acoustic waves and the nonequilibrium heat release and as a result their amplification occurs. For the laboratory media, the term "acoustic instability" is more common. As for astrophysical media, the generally accepted term is "isentropic instability." In Refs. [15,16], it was shown that the isentropic instability condition coincides with the condition of bulk viscosity being negative.

For such gaseous media as interstellar medium, the isentropic instability was first studied by Oppenheimer [17]. With the help of linear analysis, it was shown that acoustic perturbations can be unstable in the molecular zone of photodissociation regions (PDRs). The nonlinear stage of acoustic perturbation evolution was consequently considered by Krasnobaev

and Tarev [18]. Their analysis was based upon the nonlinear Burgers equation with source term derived from the initial system of gas dynamic equation (taking into account the generalized heat-loss function in the heat transfer equation). They stated that the growth of weak perturbations accompanied by nonlinear wave steepening leads to the formation of a shock wave. The derived nonlinear equation was obtained by use of high-frequency approximation $\omega\tau \gg 1$, where ω is the frequency of perturbation, and τ is the characteristic heating time. Thus, the evolution of the low-frequency part of spectrum was not taken into account. This equation has a solution in the form of traveling sawtooth waves. However, this solution is unstable with respect to waves of a larger period [19]. In addition, the sawtooth wave itself has a spectrum far beyond the high-frequency approximation (see also discussion in Sec. VIII of this article). Through numerical simulations within the model of Oppenheimer [17], Krasnobaev *et al.* [20] formulated that the single pulse tends to produce a periodic sequence of shock waves. Subsequently, this result has been confirmed analytically and numerically by Molevich *et al.* [16] in the course of the analysis of waves in the atomic surface layer of a PDR. Analytical results presented in paper [16] have been obtained on the basis of nonlinear equation obtained from the initial system of gasdynamic equations without using limitation on the perturbation frequency under weakly nonlinear approximation and the assumption of weak dispersion. This equation coincides, within the nature of coefficients, with the NAE obtained for stationary nonequilibrium media [1,5,6]. The stationary solutions of this equation in the form of traveling waves describe the decay of weak perturbations into a sequence of autowaves with a shock front. The parameters of the autowaves are determined analytically and coincide with those obtained as a result of the numerical solution of gasdynamic equations. Speaking of geometry factor, Krasnobaev [21] has shown that the plane, cylindrical, or spherical shock wave breaking into a periodic sequence of shock waves occurs irrespective of the geometry. Two-dimensional simulations by Krasnobaev [21] have suggested that the presence of multiple shocks in a thermally unstable medium accelerate significantly the destruction of preexisting isolated condensations. Numerical two-dimensional simulations of perturbation evolution in the isentropically unstable gas has been conducted in Ref. [22] as well. It has been shown that one-dimensional slices of the obtained two-dimensional wave structures coincide with solutions of NAE. The examples of observed PDRs where the isentropic instability produces multiple shock waves are given in Ref. [23].

Another example of astrophysical heat-releasing medium is the solar atmosphere. In contrast to the interstellar medium, for the given medium, it is very important to take into account influence of a magnetic field.

The structure and properties of gasdynamic perturbations in a conducting medium in the presence of magnetic field are described by a system of magnetohydrodynamic (MHD) equations. In such a medium, three types of MHD waves are possible: the Alfvén, fast, and slow magnetoacoustic (MA) waves. Slow and fast magnetoacoustic waves are compressible and susceptible to damping. Alfvén waves are transverse incompressible magnetic oscillations.

Understanding the properties of MHD waves in the solar corona is of importance not only in the context of the above-mentioned phenomenon. It attracts attention in the context of the coronal heating and solar wind acceleration problems and as a diagnostic tool of the coronal plasma via a technique called coronal seismology (see, e.g., Refs. [24,25] for recent reviews). In the last two decades, due to the development of the resolving power of measuring instruments, as well as the appearance of new spacecraft designed to analyze the dynamics of the Sun, numerous observations of MA perturbations propagating in various regions of the solar atmosphere have been made. Trains of MA waves are observed in various regions of the solar atmosphere, e.g., in coronal loops [26–30], coronal plumes [31,32], coronal holes [33,34], etc. In most papers described above, magnetoacoustic waves are seen as damped waves. This effect is quite expected since in the hot plasma of the solar atmosphere, viscosity and thermal conductivity demonstrate a significant effect on the dynamics of waves. However, despite the presence of strong dissipative processes, the undamped and even amplifying magnetoacoustic waves are observed [35–38]. The cause of this phenomenon has not been determined yet.

In papers [39–41], the reason for the amplification of MA waves (both fast and slow) has been associated with the isentropic thermal instability of plasma due to misbalance between the heat release of high-temperature plasma and radiation cooling in the course of MA perturbation propagation. With the help of data from the CHIANTI atomic database and the available solar corona heating models, it was shown in Refs. [42–44], that isentropically unstable regions may exist in the solar corona and can be one of the reasons of long-lived undamped trains of magnetoacoustic waves. The regions of isentropic instabilities in solar corona has been also obtained in Refs. [45,46] with the help of modern data about heat-loss function. In the case of isentropic instability the mutual effect of the wave amplification and dispersion is shown to result in the occurrence of an oscillatory pattern in an initially broadband slow wave, with the characteristic period determined by the thermal misbalance time scales (derivatives of the heat-loss function) [45]. In general case, the thermal misbalance (term used for generalization of various thermal instabilities/stabilities) have many different regimes. The comparison of the observed and theoretically derived amplification/decay times and oscillation periods allows one to constrain the coronal heating function. For typical coronal parameters, the observed properties of standing slow magnetoacoustic oscillations could be readily reproduced with a reasonable choice of the heating function [46].

Interest in the nonlinear stage of isentropic instability in application to the solar atmosphere has existed for more than 10 years [39–41], since at this stage the formation of self-sustaining waves is possible. Such waves are defined by internal processes of the medium only and can give plentiful information about these processes. Particularly, it has been proposed to investigate the nonlinear evolution of waves using the Burgers equation with the nonlinear source term [39]. As a result, it was shown that formation of undamped trains of magnetoacoustic autowaves in solar atmosphere condition may take place. However, it should be noted that the introduced equation itself has also been obtained in the high-

frequency limit and autowave structures described by this equation have a spectrum wider than a considered frequency range.

In the present work, we mean to obtain the nonlinear magnetoacoustic equation (NMAE) which is capable to describe the evolution of nonlinear waves without limiting the acoustic spectrum like the previously mentioned NAE. Subsequently, the obtained equation is used for a detailed theoretical study of nonlinear fast and slow MA waves.

Layout of the paper is as follows. In Sec. II the initial MHD model taking into account the heat-loss function Q is discussed. Further, in Sec. III we carry out a linear analysis of acoustic waves and introduce an approach used for the description of specific dispersion properties of waves. Then in Sec. IV the introduced approach is applied to the description of dispersion properties of MA waves and the definition of wave phase velocity and increment/decrement. In Sec. V we derive the nonlinear magnetoacoustic equation (NMAE) for fast and slow MA waves and discuss its coefficients. Further, in Sec. VI we define the stationary solutions of NMAE in the form of shock waves of different profiles and in the form of autowave pulse in the medium with isentropic instability. In Sec. VII to validate the evolutionary stability of the theoretically predicted structures, the numerical simulations of NMAE (Sec. VII A) and the system of one-dimensional MHD equations (Sec. VII B) are performed. The instability of weak MA shock waves to the decay into trains of autowave impulses is shown. Finally, in Sec. VIII we compare the NMAE with existing nonlinear equations and discuss our main results.

II. MODEL AND ASSUMPTIONS

To begin with, let us specify the governing equations and assumptions used for the analysis of the nonadiabatic effects caused by the unbalance between the heat release of the high-temperature plasma and the radiation cooling. The plasma is assumed to be in thermodynamic equilibrium. We consider waves with timescales much larger than the collision times and length scales much longer than the mean-free paths. The plasma under consideration is also assumed to be uniform, quasineutral, and fully ionized. Plasma permeability and permittivity are equal to unity. We exclude the influence of self-gravitation, steady flows effects, and dissipation caused by the viscosity and finite electrical conduction. Nevertheless, the weak dissipation is taken into account in the form of the thermal conduction. However, we ignore the temperature dependence of the thermal conduction coefficient. With the foregoing as background, the governing set of MHD equations is written as follows:

$$\frac{\partial \boldsymbol{B}}{\partial t} = \mathrm{rot}[\boldsymbol{V} \times \boldsymbol{B}],$$

$$\mathrm{div}\boldsymbol{B} = 0, \quad \frac{\partial \rho}{\partial t} + \mathrm{div}\rho\boldsymbol{V} = 0,$$

$$\rho\frac{d\boldsymbol{V}}{dt} = -\boldsymbol{\nabla}P - \frac{1}{4\pi}[\boldsymbol{B} \times \mathrm{rot}\boldsymbol{B}], \quad P = \frac{k_B}{m}\rho T, \quad (6)$$

$$C_{V\infty}\frac{dT}{dt} - \frac{k_B T}{m\rho}\frac{d\rho}{dt} = -Q(\rho, T) + \frac{1}{\rho}\boldsymbol{\nabla}(\kappa\boldsymbol{\nabla}T),$$
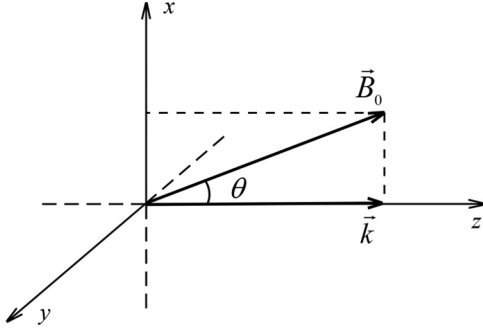
$$Q(\rho, T) = L(\rho, T) - H(\rho, T),$$

FIG. 1. Wave propagation scheme. The direction of the wave propagation is along the wave vector $\boldsymbol{k}$. The direction of the external magnetic field is along the vector $\boldsymbol{B_0}$.

where ρ is the plasma density, T is the temperature, P is the plasma pressure, $\boldsymbol{V}$ and $\boldsymbol{B}$ are the velocity and magnetic field vectors, respectively. We also use some standard notations: k_B is the Boltzmann constant, κ is the thermal conductivity, m is the mean particle mass, and $C_{V\infty}$ is the specific heat at constant volume. The introduction reason of additional index "∞" in the specific heat coefficient will be clarified in Sec. III. The system of Eqs. (6) is written in the CGS system of units using the substantial derivative ($d/dt = \partial/\partial t + \boldsymbol{V}\nabla$).

To conduct the analysis of the wave dynamics, we use the Cartesian coordinate system x, y, z. We assume that waves propagate along z axis and the vector of external uniform magnetic field lies in the x-z plane (i.e. $\boldsymbol{B_0} = B_0 \sin\theta \boldsymbol{x_0} + B_0 \cos\theta \boldsymbol{z_0}$, where B_0 is the absolute value of the magnetic field vector, θ is the angle between vector $\boldsymbol{B_0}$ and z axis, $\boldsymbol{x_0}$ and $\boldsymbol{z_0}$ are unit vectors) (see Fig. 1). The dependencies of variables on coordinates x and y are neglected ($\partial/\partial x = \partial/\partial y = 0$)

III. LINEAR APPROACH: DISPERSION RELATIONS FOR ACOUSTIC WAVES

Before we start the nonlinear analysis of wave properties, the linear analysis of the waves properties has to be done. We seek a solution of the linearized system of Eqs. (6) using the following substitution:

$$a(z, t) = a_0 + a_1(z, t).$$

Hereinafter, the quantity a means any variable (density, temperature, pressure, etc.) describing the state of the medium. Subscript "0" means the unperturbed medium state, numeric subscript ("1", "2", etc.) means the order of smallness ($a_1/a_0 \sim \epsilon$, $a_2/a_0 \sim \epsilon^2$, where $\epsilon \ll 1$), alphabetic subscripts ("x", "y", "z") mean the corresponding component of the vector:

$$\frac{\rho_1}{\rho_0} \sim \frac{P_1}{P_0} \sim \frac{T_1}{T_0} \sim \frac{B_{1x}}{B_0} \sim \frac{B_{1y}}{B_0} \sim \frac{B_{1z}}{B_0} \sim \frac{V_{1x}}{c_\infty}$$

$$\sim \frac{V_{1y}}{c_\infty} \sim \frac{V_{1z}}{c_\infty} \sim \epsilon \ll 1.$$

The alphabetic subscript after the comma or round brackets means the corresponding partial derivative (see examples below):

$$a_{1,z} = \frac{\partial a_1}{\partial z}, \quad a_{1x,t} = \frac{\partial a_{1x}}{\partial t}, \quad a_{2,tz} = (a_{2,t})_z = \frac{\partial^2 a_2}{\partial t \partial z}.$$

To start the discussion about the influence of nonadiabatic processes on MA waves, a few words should be said about the approach used in the current research.

It is well known [6,47,48] that the nonadiabatic processes caused by the misbalance between the heat release and the radiation cooling significantly affect the dispersion properties of the waves in the medium. The description of these properties can be given in the different ways. Particularly, the introduction of characteristic scales and dimensionless parameters has been used in the analysis of waves propagating in the gaseous [49] and plasma [44,50] media conducted by Ibanez *et al.* Another approach, applied in Ref. [13], is the introduction of characteristic frequencies. A significant drawback of these approaches is the unwieldiness of the formulas and the lack of a physical sense in a number of the notations introduced.

In the current research, we use another approach based on the analogy with the nonequilibrium relaxing medium. This analogy had been mentioned for the first time in Ref. [15] and subsequently has been developed and used during the analysis of waves in the interstellar medium [16]. The detailed description of the wave properties in the nonequilibrium relaxing medium can be found in Refs. [51,52]. According to the theory presented in Refs. [51,52], distortions of gas-dynamic flows caused by the nonequilibrium processes are primarily attributable to changes in the specific heats and in the effective adiabatic index γ_{eff} of the nonequilibrium gas, on which the gas-dynamic process depends. Therefore, in the current research, to describe the influence of the misbalance between the heat release of the high-temperature plasma and the radiation cooling during the propagation of gas-dynamic perturbations, we have introduced the low-frequency specific heats at constant volume C_{V0} and at constant pressure C_{P0} by analogy with the equilibrium specific heats in the relaxing media [2,15,51,52]. The standard expressions for specific heats at constant volume C_V and at constant pressure C_P in this approach are denoted by the high-frequency specific heats $C_{V\infty}$ and $C_{P\infty}$, respectively.

To demonstrate the main advantages of this approach and introduce some basic notations that will be used later, we first consider and describe the dispersion properties of pure acoustic waves in the ideal thermally unstable gas. The system of equations describing these waves can be obtained from the system of Eqs. (6), neglecting all magnetic effects and heat conductivity. The application of the mentioned approach to the linearization procedure and substitution of the harmonic wave solution $\sim \exp(-i\omega t + ikz)$ (where ω is the frequency and k is the wave number) into the linearized system of Eqs. (6) describing pure acoustic waves, gives us the following dispersion relation:

$$\tilde{c}^2 = \frac{\omega^2}{k^2} = \frac{(C_{P0} - i\omega\tau_0 C_{P\infty})}{(C_{V0} - i\omega\tau_0 C_{V\infty})} \frac{k_B T_0}{m} = \gamma_{\text{eff}} \frac{k_B T_0}{m}, \quad (7)$$

where

$$\tau_0 = \frac{k_B T_0}{m H_0} \quad (8)$$

and

$$C_{P\infty} = C_{V\infty} + \frac{k_B}{m}, \quad C_{V0} = Q_{0T}\tau_0 = \frac{k_B}{m}Q_{L0T},$$

$$C_{P0} = \tau_0(Q_{0T}T_0 - Q_{0\rho}\rho_0)/T_0 = \frac{k_B}{m}(Q_{L0T} - Q_{L0\rho}),$$

$$Q_{0T} = \left(\frac{\partial Q}{\partial T}\right)\Big|_{\rho_0, T_0}, \quad Q_{0\rho} = \left(\frac{\partial Q}{\partial \rho}\right)\Big|_{\rho_0, T_0},$$

$$Q_{L0T} = \frac{T_0 Q_{0T}}{H_0}, \quad Q_{L0\rho} = \frac{\rho_0 Q_{0\rho}}{H_0}. \tag{9}$$

Hereinafter, we consider the spatial amplification (or attenuation) of waves, that is, we assume the wave vector to be complex $k = \operatorname{Re} k + i \operatorname{Im} k$, and the frequency ω to be real. The case of negativity of the imaginary part of the wave vector will correspond to the amplification.

The first advantage of this approach following from Eqs. (9) is that the positive/negative sign of the low-frequency specific heats at constant volume C_{V0} and at constant pressure C_{P0} coincides with the conditions of isochoric and isobaric stability/instability, respectively. Thus, it can be easily seen the influence of the definite instability type on the dispersion properties of waves (7).

Using notations (9), the isochoric, isobaric and isentropic instability conditions (3)–(5) can be rewritten, respectively, as follows:

$$C_{V0} < 0, \tag{10}$$

$$C_{P0} < 0, \tag{11}$$

$$(\gamma_\infty - \gamma_0)/C_{V0} < 0. \tag{12}$$

The next advantage of this approach is expressed in the simplicity and clarity of the way to describe the frequency dependence of the wave characteristics.

Indeed, the solution of dispersion relation (7), found using the assumption of weak amplification/attenuation at the wavelength ($\operatorname{Im} k \ll \operatorname{Re} k$), gives the frequency dependence of the phase velocity, written explicitly in terms of the speeds of low- and high-frequency perturbations:

$$c_{Snd}(\omega) = \frac{\omega}{\operatorname{Re} k} = \sqrt{\frac{\left(C_{V0}^2 c_0^2 + \omega^2 \tau_0^2 C_{V\infty}^2 c_\infty^2\right)}{\left(C_{V0}^2 + \omega^2 \tau_0^2 C_{V\infty}^2\right)}}, \tag{13}$$

where

$$c_\infty = \sqrt{\gamma_\infty \frac{k_B T_0}{m}}, \quad c_0 = \sqrt{\gamma_0 \frac{k_B T_0}{m}}, \tag{14}$$

$$\gamma_\infty = \frac{C_{P\infty}}{C_{V\infty}}, \quad \gamma_0 = \frac{C_{P0}}{C_{V0}} = \frac{Q_{L0T} - Q_{L0\rho}}{Q_{L0T}}. \tag{15}$$

Here special attention should be given to the important parameter which defines the frequency dependence of the acoustic perturbations, namely, the characteristic heating/cooling time τ_0 (8). This parameter allows us to subdivide the whole frequency spectrum into two qualitatively different ranges. In the high-frequency range ($\omega\tau_0 \gg 1$), the phase velocity of the acoustic perturbations $c_{Snd(\omega\tau_0 \gg 1)} = c_\infty$ (14), while in the low-frequency range ($\omega\tau_0 \ll 1$), the phase velocity is defined by the thermal misbalance only $c_{Snd(\omega\tau_0 \ll 1)} = c_0$ (14).

The appearance of a low-frequency adiabatic coefficient γ_0 in form (15) in heat-releasing gas media was discussed earlier in Ref. [15], and it follows directly from the heat equation. Indeed, for small perturbations of pressure and density, we can write this equation in a linearized form:

$$C_{V\infty} \frac{\partial P_1}{\partial t} - C_{P\infty} \frac{k_B T_0}{m} \frac{\partial \rho_1}{\partial t} = -[Q_{0T} P_1 + (Q_{0\rho} \rho_0 - Q_{0T} P_0)\rho_1]. \tag{16}$$

Or, taking into account the above notations, we obtain

$$C_{V\infty} \tau_0 \left(\frac{\partial P_1}{\partial t} - \gamma_\infty \frac{k_B T_0}{m} \frac{\partial \rho_1}{\partial t}\right) = -C_{V0}\left[P_1 - \gamma_0 \frac{k_B T_0}{m} \rho_1\right]. \tag{17}$$

From (17), it follows that in the high-frequency range ($\omega\tau_0 \gg 1$)

$$\tau_0 \frac{\partial a_1}{\partial t} \to \infty,$$

we have

$$P_1 = \gamma_\infty \frac{k_B T_0}{m} \rho_1 = c_\infty^2 \rho_1. \tag{18}$$

In the opposite case, namely, in the low-frequency limit ($\omega\tau_0 \ll 1$)

$$\tau_0 \frac{\partial a_1}{\partial t} \to 0,$$

the relation between linear perturbations of pressure and density has another form:

$$P_1 = \gamma_0 \frac{k_B T_0}{m} \rho_1 = c_0^2 \rho_1. \tag{19}$$

Thus, the adiabatic indices and the sound speeds determined by them essentially depend on the frequency range of the acoustic perturbation. In a simple form (from the point of view of physical interpretation), one can also write the frequency dependence of the increment/decrement of waves, obtained from (7):

$$\alpha = \operatorname{Im} k = \frac{\omega^2 \xi(\omega)}{2\rho_0 c_{Snd}^3(\omega)}, \tag{20}$$

$$\xi = \frac{\xi_0 C_{V0}^2}{C_{V0}^2 + \omega^2 \tau_0^2 C_{V\infty}^2};$$

$$\xi_0 = \frac{\rho_0 \tau_0 C_{V\infty}(c_\infty^2 - c_0^2)}{C_{V0}}$$

$$= \frac{P_0 \tau_0(Q_{L0\rho}/(\gamma_\infty - 1) + Q_{L0T})}{Q_{L0T}^2}, \tag{21}$$

where ξ is the bulk viscosity coefficient and ξ_0 is the bulk viscosity coefficient in the low-frequency limit [15,16].

It would not be superfluous to mention that, according to Ref. [52], the presence of slow processes tending to establish equilibrium is macroscopically equivalent to the presence of a bulk viscosity. In the case under study, slow processes are heating and cooling both characterized by time τ_0 in the medium under investigation.

According to (20) and (21), the amplification condition is the condition of the negative bulk viscosity or, equivalently, isentropic instability condition (5) and (12). If this condition is satisfied, the positive feedback between the nonadiabatic processes and acoustic perturbations takes place.

IV. DISPERSION RELATIONS FOR MAGNETOACOUSTIC WAVES

Let us return to the study of the features of the propagation of MHD waves in heat-releasing media.

The thermal mode and three types of MHD waves are described by system (6), namely, the Alfvén wave and fast and slow magnetoacoustic waves. Alfvén waves propagate without compression of the medium (only transversal y components of the velocity and magnetic field vectors are perturbed). Linear analysis of system of Eqs. (6) gives an evolutionary equation for Alfvén waves in the following form:

$$B_{1y,tt} - c_{az}^2 B_{1y,zz} = 0, \tag{22}$$

where $c_{az}^2 = c_a^2 \cos^2 \alpha$; $c_a^2 = B_0^2/4\pi\rho_0$; c_a is the Alfvén speed. As can be seen from Eq. (22), the presence of heating and cooling does not affect the stability of this type of waves.

Another situation develops with magnetoacoustic waves. In the linear approximation, using the low-frequency and high-frequency specific heats and sound speeds introduced in Sec. III, we can easily obtain the linear evolutionary equation describing the propagation of the fast and slow magnetoacoustic waves and the thermal wave in the following form:

$$C_{V\infty}\tau_0 \big[B_{1x,tttt} - (c_a^2 + c_\infty^2)B_{1x,ttzz} + c_\infty^2 c_{az}^2 B_{1x,zzzz} \big]_t$$
$$+ C_{V0}\big[B_{1x,tttt} - (c_a^2 + c_0^2)B_{1x,ttzz} + c_0^2 c_{az}^2 B_{1x,zzzz} \big]$$
$$= \frac{\kappa_z \tau_0}{\rho_0} \big[B_{1x,tttt} - (c_a^2 + c_T^2)B_{1x,ttzz} + c_T^2 c_{az}^2 B_{1x,zzzz} \big]_{zz}. \tag{23}$$

The implicit dispersion relation for these modes can be written as follows:

$$C_{V\infty}\tau_0(-i\omega)\big[\omega^4 - (c_a^2 + c_\infty^2)\omega^2 k^2 + c_\infty^2 c_{az}^2 k^4 \big]$$
$$+ C_{V0}\big[\omega^4 - (c_a^2 + c_0^2)\omega^2 k^2 + c_0^2 c_{az}^2 k^4 \big]$$
$$+ \frac{\kappa_z \tau_0}{\rho_0}(k^2)\big[\omega^4 - (c_a^2 + c_T^2)\omega^2 k^2 + c_T^2 c_{az}^2 k^4 \big] = 0. \tag{24}$$

Here $c_T = \sqrt{k_B T_0/m}$ is the isothermal speed of sound, $\kappa_z = \kappa_\parallel \cos^2 \theta + \kappa_\perp \sin^2 \theta$ is the component of the thermal conduction coefficient along the z axis, $\kappa_\parallel$ and $\kappa_\perp$ are the thermal conduction coefficients along and across a magnetic field, respectively.

If we assume that thermal conduction is weak, the reduction of this dispersion equation gives us simpler dispersion relations for thermal and MA waves, respectively:

$$k^2 = -\frac{\rho_0(C_{P0} - i\omega\tau_0 C_{P\infty})}{\kappa_z m \tau_0}, \tag{25}$$

$$\frac{\omega^2}{k^2} = \frac{(c_a^2 + \tilde{c}^2) \pm \sqrt{(c_a^2 + \tilde{c}^2)^2 - 4c_{az}^2 \tilde{c}^2}}{2}, \tag{26}$$

where "+" corresponds to the fast MA wave, and "−" corresponds to the slow MA wave.

According to (25), the thermal wave always damps during propagation in the medium with isobaric stability. Thus, it will not be investigated further in this article.

If we neglect the effect of a misbalance or consider only high-frequency perturbations ($\omega\tau_0 \gg 1$), the complex speed (7) becomes equal to the high-frequency expression $\tilde{c}^2 = c_\infty^2$

and dispersion relation (26) is reduced to the well-known relation for MA waves in the equilibrium medium [53].

As before, we obtain the frequency dependent phase velocity of MA waves $c_{f,s}(\omega)$ and the increment/decrement of MA waves $\alpha_{f,s}(\omega)$ assuming weak amplification/attenuation of the waves at the wavelength (Im $k \ll$ Re k):

$$c_{f,s}(\omega) = \frac{\omega}{\text{Re}\,k}$$
$$= \sqrt{\frac{(c_a^2 + c_{Snd}^2) \pm \sqrt{(c_a^2 + c_{Snd}^2)^2 - 4c_{az}^2 c_{Snd}^2}}{2}}, \tag{27}$$

$$\alpha_{f,s}(\omega) = \text{Im}\,k = \frac{\omega^2 \xi}{4\rho_0 c_{f,s}^3}\,\Xi_{Snd}, \tag{28}$$

where

$$\Xi_{Snd}(\omega) = 2\frac{c_{f,s}^2 - c_a^2 \cos^2 \theta}{2c_{f,s}^2 - [c_a^2 + c_{Snd}^2]}$$
$$= \left(1 \pm \frac{c_{Snd}^2 - c_a^2 \cos 2\theta}{\sqrt{c_{Snd}^4 + c_a^4 - 2c_{Snd}^2 c_a^2 \cos 2\theta}} \right).$$

Hereinafter, indices "f" and "s" correspond to the fast and slow MA waves, respectively. The bulk viscosity coefficient ξ is defined in Sec. III.

The nonadiabatic processes affect MA waves in a manner identical to that for the pure acoustic waves. In the high-frequency range ($\omega\tau_0 \gg 1$), the phase velocity of the MA waves is defined by the well-known expression for the equilibrium medium $c_{f,s(\omega\tau_0 \gg 1)} = c_{\infty f,s}$, while in the low-frequency range ($\omega\tau_0 \ll 1$), the phase velocity is defined by the nonadiabatic processes $c_{f,s(\omega\tau_0 \ll 1)} = c_{0f,s}$. These phase velocities are easily defined by the passage to the high- and low-frequency limits:

$$c_{0f,s} = \sqrt{0.5\big[c_a^2 + c_0^2 \pm \sqrt{(c_a^2 + c_0^2)^2 - 4c_{az}^2 c_0^2} \big]},$$
$$c_{\infty f,s} = \sqrt{0.5\big[c_a^2 + c_\infty^2 \pm \sqrt{(c_a^2 + c_\infty^2)^2 - 4c_{az}^2 c_\infty^2} \big]}. \tag{29}$$

The expression (28) enables us to determine the condition of MA wave amplification. All quantities in expression (28) are positive for all possible wave propagation directions and values of magnetic field strength except for the bulk viscosity coefficient. Therefore, the amplification condition for both fast and slow MA wave is, as for acoustic waves, the condition of the negative bulk viscosity or, equivalently, isentropic instability condition (12).

The increment/decrement of MA waves as well as the increment/decrement of pure acoustic waves [16] is frequency dependent. Both the high- and low-frequency limits of the MA wave increment/decrement are as follows:

$$\alpha_{0f,s} = \frac{\omega^2 \xi_0}{4\rho_0 c_{0f,s}^3}\,\Xi_0, \quad \alpha_{\infty f,s} = \frac{\xi_0 C_{V0}^2}{4\rho_0 c_{\infty f,s}^3 \tau_0^2 C_{V\infty}^2}\,\Xi_\infty, \tag{30}$$

where

$$\Xi_0 = 2\frac{c_{0f,s}^2 - c_a^2 \cos^2 \theta}{2c_{0f,s}^2 - [c_a^2 + c_0^2]}, \quad \Xi_\infty = 2\frac{c_{\infty f,s}^2 - c_a^2 \cos^2 \theta}{2c_{\infty f,s}^2 - [c_a^2 + c_\infty^2]}.$$
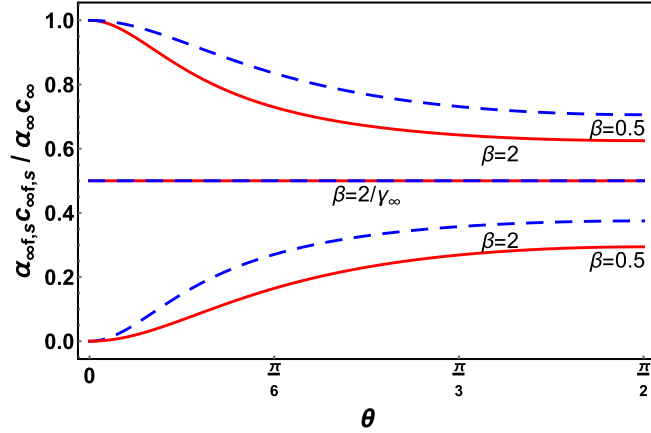
FIG. 2. Dependences of normalized increment on angle between the magnetic field vector and the propagation direction for beta equal to 2, 0.5, and $2/\gamma_\infty$. Red solid lines correspond to fast magnetoacoustic waves. Blue dashed lines correspond to slow magnetoacoustic waves.
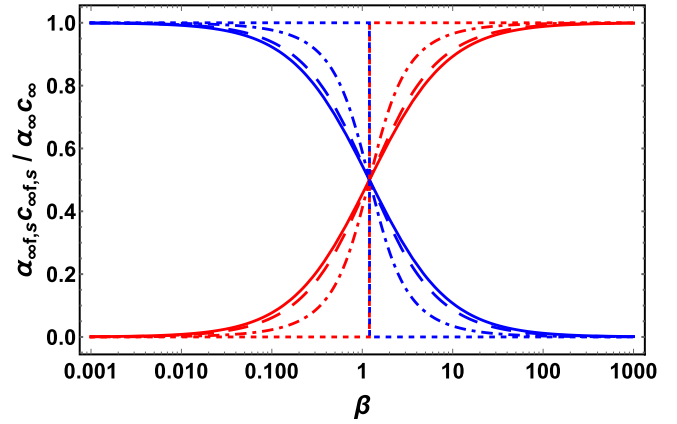

FIG. 3. Dependences of normalized increment on plasma beta. Red and blue colors correspond to fast and slow magnetoacoustic waves, respectively. Solid lines, $\theta = \pi/2$; dashed lines, $\theta = \pi/3$; dot-dashed lines, $\theta = \pi/6$; dotted line, $\theta = 0$.

One can notice that in the low-frequency limit ($\omega\tau_0 \ll 1$), the spatial increment $\mathrm{Im}\,k$ of the MA waves depends on frequency quadratically $\sim\omega^2$, while in the high-frequency limit ($\omega\tau_0 \gg 1$) it is frequency independent, as it is for the pure acoustic waves. This is the consequence of the bulk viscosity frequency dependence.

In contrast with the pure acoustic waves, the MA waves cause not only the pressure perturbation but also result in the magnetic tension disturbance. In order to characterize the magnetic field strength, we will use the well-known dimensionless parameter, namely, so-called beta of plasma:

$$\beta = \frac{8\pi P_0}{B_0^2} = \frac{2}{\gamma_\infty}\frac{c_\infty^2}{c_a^2}. \tag{31}$$

This parameter is the ratio of the plasma pressure to the magnetic pressure. The term "beta" is commonly used in the astrophysics and in the field of the controlled thermonuclear fusion.

Moreover, it is to be noted that MA waves are anisotropic. Considering this anisotropy, one can show that slow magnetoacoustic waves as well as Alfvén waves do not propagate across the external magnetic field. In contrast to these waves, the fast magnetoacoustic waves can propagate in all possible directions.

It is also essential to discuss the anisotropy of the MA wave increment/decrement. To show the dependence of MA waves increment on plasma beta and the direction of the external magnetic field, we plot the dimensionless quantities $\alpha_{\infty f}c_{\infty f}/a_\infty c_\infty$, $\alpha_{\infty s}c_{\infty s}/a_\infty c_\infty$ (see Fig. 2). Using these quantities, we exclude the ambiguity in some limit cases. Here we use the high-frequency increment of pure acoustic waves in the following form:

$$\alpha_\infty = \frac{\xi_0 C_{V0}^2}{2\rho_0 c_\infty^3 \tau_0^2 C_{V\infty}^2}. \tag{32}$$

The plots in Figs. 2 and 3 show that amplification of the fast MA waves independently on propagation direction is greater than amplification of the slow MA waves in the high-

beta plasma. In the low-beta plasma, the opposite situation occurs. They also show that in the case of $\beta = 2/\gamma_\infty \sim 1$ both increments for fast and slow MA waves equal to half of the pure acoustic wave increment.

Considering the case when amplification dominates over the dissipation, the linear equation becomes useless for the description of the stationary wave structures. That is because it can predict only the infinite growth of the perturbations. This problem can be solved by the taking into account the quantities of the higher order of smallness. We will clarify this question in the following section.

V. NONLINEAR MAGNETOACOUSTIC EQUATION

The uncompensated isentropic instability restricts the applicability of linear Eq. (23). As we will show further, for a stabilization of the isentropic instability to be reached, the inclusion of quadratic nonlinear terms is sufficient. In other words, the formation of the stationary wave structures can be described by the nonlinear equation obtained for the finite amplitude perturbations within the accuracy up to terms of the second order of smallness $\sim\epsilon^2$, $\epsilon \ll 1$. In this section, we give the detailed description of this equation. The main steps of its derivation are briefly discussed in the Appendix.

Here we should point out only that this equation has been obtained by using the assumptions of the weak dispersion and dissipation:

$$\frac{|c_0^2 - c_\infty^2|}{c_\infty^2} \sim \epsilon \ll 1, \qquad \frac{\kappa_z}{\rho_0 T_0 \tau_0} \sim \epsilon \ll 1.$$

It is well known that the MA waves are the compression waves. Therefore, we found it convenient to define the nonlinear equation as an equation describing the density perturbation. Nevertheless, the way of transformation to the other variables can be found in the Appendix. For a subsequent analysis of this equation to perform, it seems appropriate to use dimensionless variables $\tilde{\rho} = \rho_1/\rho_0$. Due to the fact that we are interested in the analysis of stationary wave structures, we also use the assumption of the slowly varying wave

profile and introduce the following dimensionless change of coordinates: $\tilde{\xi} = (z - c_{\infty f,s} t)/c_{\infty f,s}\tau_0$, $\tilde{\tau} = \epsilon t/\tau_0$.

With the foregoing as background, the nonlinear equation for the fast and slow magnetoacoustic waves can be written as follows:

$$\frac{\partial}{\partial \tilde{\xi}}\left(\frac{\partial \tilde{\rho}}{\partial \tilde{\tau}} + \frac{\Psi_\infty}{2}\frac{\partial \tilde{\rho}^2}{\partial \tilde{\xi}} - \mu_\infty \frac{\partial^2 \tilde{\rho}}{\partial \tilde{\xi}^2}\right)$$
$$- \nu\left(\frac{\partial \tilde{\rho}}{\partial \tilde{\tau}} + \frac{\tilde{m}}{2}\frac{\partial \tilde{\rho}}{\partial \tilde{\xi}} + \frac{\Psi_0}{2}\frac{\partial \tilde{\rho}^2}{\partial \tilde{\xi}}\right) = 0, \qquad (33)$$

where the coefficients are given as follows:

$$\Psi_\infty = \left(\frac{\gamma_\infty + 1}{2}\right)\frac{\gamma_\infty}{\gamma_{\infty f,s}}\frac{(\gamma_{\infty f,s} - \gamma_a \cos^2\theta)}{(2\gamma_{\infty f,s} - \gamma_a - \gamma_\infty)}$$
$$+ \frac{3}{2}\frac{(\gamma_{\infty f,s} - \gamma_\infty)}{(2\gamma_{\infty f,s} - \gamma_a - \gamma_\infty)}, \qquad (34)$$

$$\Psi_0 = \left(\frac{2\gamma_0 - 1}{\gamma_{0f,s}}\right)\frac{(\gamma_{0f,s} - \gamma_a \cos^2\theta)}{(2\gamma_{0f,s} - \gamma_a - \gamma_0)} + \frac{3}{2}\frac{(\gamma_{0f,s} - \gamma_0)}{(2\gamma_{0f,s} - \gamma_a - \gamma_0)}$$
$$- \frac{1}{2Q_{L0T}}\frac{(\gamma_{0f,s} - \gamma_a \cos^2\theta)}{\gamma_{0f,s}(2\gamma_{0f,s} - \gamma_a - \gamma_0)}$$
$$\times (Q_{L0\rho\rho} + Q_{L0TT}(\gamma_0 - 1)^2 + 2Q_{L0\rho T}(\gamma_0 - 1)), \quad (35)$$

$$\mu_\infty = \left[\frac{1}{\tau_0 c_{S\infty}^2}\frac{\kappa_z m}{\rho_0 k_B}\right]\frac{(\gamma_\infty - 1)^2}{\gamma_{\infty f,s}} \times \frac{(\gamma_{\infty f,s} - \gamma_a \cos^2\theta)}{2(2\gamma_{\infty f,s} - \gamma_a - \gamma_\infty)}, \qquad (36)$$

$$\tilde{m} = \frac{(\gamma_0 - \gamma_\infty)}{\gamma_\infty}\frac{(\gamma_{0f,s} - \gamma_a)}{(2\gamma_{0f,s} - \gamma_a - \gamma_0)}, \qquad (37)$$

$$\nu = \frac{C_{V0}}{C_{V\infty}}. \qquad (38)$$

We also introduce some notations for description convenience $\gamma_{\infty f,s} = c_{\infty f,s}^2/c_T^2$, $\gamma_{0f,s} = c_{0f,s}^2/c_T^2$, $\gamma_a = c_a^2/c_T^2$:

$$\gamma_{\infty f,s} = \frac{(\gamma_a + \gamma_\infty) \pm \sqrt{(\gamma_a + \gamma_\infty)^2 - 4\gamma_\infty \gamma_a \cos^2\theta}}{2},$$

$$\gamma_{0f,s} = \frac{(\gamma_a + \gamma_0) \pm \sqrt{(\gamma_a + \gamma_0)^2 - 4\gamma_0 \gamma_a \cos^2\theta}}{2}, \quad (39)$$

$$\gamma_a = \frac{2}{\beta},$$

and

$$Q_{L0TT} = \frac{T_0^2}{H_0}\left(\frac{\partial^2 Q}{\partial T^2}\right)\bigg|_{\rho_0, T_0},$$

$$Q_{L0\rho\rho} = \frac{\rho_0^2}{H_0}\left(\frac{\partial^2 Q}{\partial \rho^2}\right)\bigg|_{\rho_0, T_0}, \qquad (40)$$

$$Q_{L0\rho T} = \frac{\rho_0 T_0}{H_0}\left(\frac{\partial^2 Q}{\partial \rho \partial T}\right)\bigg|_{\rho_0, T_0}.$$

Now, a few words should be said about the structuring of Eq. (33) and its coefficients (34)–(38). Due to the fact that the difference between the equations for fast and slow MA waves is expressed only in the difference of coefficients, we will further speak about one nonlinear MA equation (NMAE) implying both equations for fast and slow MA waves.

The form of the nonlinear MA Eq. (33) coincides with the form of the general nonlinear acoustical equations (NAE) describing the wave evolution in the nonequilibrium relaxing gas and thermally unstable gas [1,16]. One of the most important feature of Eq. (33) is the simultaneous inclusion of the high-frequency nonlinearity coefficient Ψ_∞ (34) defined by the system of MHD equations without the heat-loss function and the low-frequency nonlinearity coefficient Ψ_0 (35) defined by the nonadiabatic processes.

Coefficient Ψ_∞ (34) coincides with the previously obtained one in Ref. [39]. In the absence of the magnetic field, it is reduced to the well-known form for the gaseous media $\Psi_{\infty\_ac} = (\gamma_\infty + 1)/2$.

In the low-frequency range ($\omega\tau_0 \ll 1$), the speed of nonlinear processes is defined mainly by the nonadiabatic processes. For the first time, coefficient Ψ_0 (35) has been obtained in Refs. [54,55]. In the absence of the magnetic field, it is also reduced to the previously obtained coefficient Ψ_{0_ac} for the gaseous media [6,16]:

$$\Psi_{0\_ac} = \frac{2\gamma_0 - 1}{\gamma_0} - \frac{1}{2\gamma_0 Q_{L0T}}[Q_{L0\rho\rho} + Q_{L0TT}(\gamma_0 - 1)^2 + 2Q_{L0\rho T}(\gamma_0 - 1)]. \qquad (41)$$

The significant difference of the low-frequency coefficient Ψ_0 (35) from the high-frequency coefficient Ψ_∞ (34) is that, in the general case, it can have not only positive but also negative sign. Because of the anisotropy of MA wave phase speeds, the nonlinear coefficients Ψ_∞ and Ψ_0 are also anisotropic.

The coefficient $\tilde{m}$ (37) characterizes the strength of the dispersion in the medium and possible amplification of waves. The functional dependence of this coefficient on the propagation direction and the plasma beta is analogous to the dependence of increment/decrement $\alpha_{\infty f,s}$(see Figs. 2 and 3). In the limit of infinitely small magnetic field, it is also reduced to the dispersion coefficient found for the pure acoustic waves [16]:

$$m_{ac} = \frac{(\gamma_0 - \gamma_\infty)}{\gamma_\infty}. \qquad (42)$$

We emphasize that the dispersion coefficient $\tilde{m}$ is positive in the conditions of isentropic instability and, simultaneously, isochoric stability. A positive coefficient $\tilde{m}$ corresponds to a negative dispersion, when the low-frequency sound velocity exceeds the velocity of high-frequency sound.

The dissipation coefficient μ_∞ (36) corresponds to the dissipation caused by the weak thermal conduction. Taking into account the difference in the definition of variables, it coincides with the expression presented in Ref. [39].

VI. POSSIBLE SOLUTIONS OF THE NMAE

The main goal of this section is to provide the detailed description of the possible solutions defined by the obtained nonlinear magnetoacoustic equation (NMAE). As we have already mentioned, the form of the NMAE equation coincides with the form of the NAE describing acoustical waves in the nonequilibrium relaxing media [1]. Analytical solution of the NAE and full classification of all possible wave structures to be described can be found in Refs. [5,56]. However, for
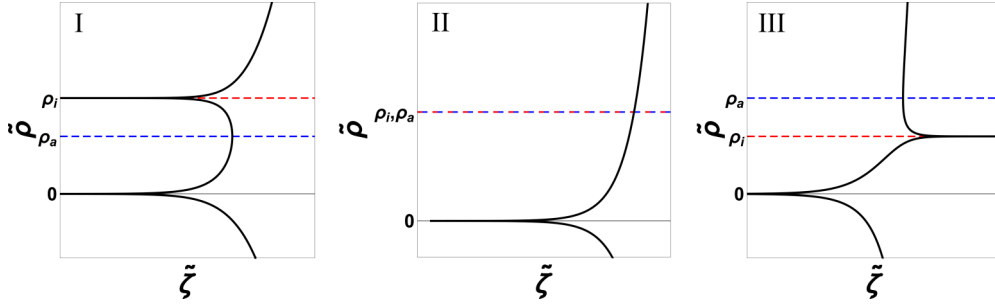
FIG. 4. Integral curves I, II, and III, described by Eq. (33) corresponding to three domains of introduced parameters ($\rho_i > \rho_a$, $\rho_i = \rho_a$, and $\rho_i < \rho_a$), respectively.

the completeness of the current research, we will describe the most important types of the wave structures which can exist in the medium with isentropic instability. Then, we show the significant differences of the obtained magnetoacoustic structures from the acoustic structures.

First, we should reduce Eq. (33) to the form which enables us to describe the stationary waves propagating with speed $D = c_{\infty f,s} + w$. In order to complete this, we use the following automodel change of variables $\tilde{\zeta} = \tilde{\xi} - w\tilde{\tau}$:

$$\mu_\infty \frac{\partial^2 \tilde{\rho}}{\partial \tilde{\zeta}^2} + \frac{\partial \tilde{\rho}}{\partial \tilde{\zeta}}(w - \Psi_\infty \tilde{\rho})$$
$$+ \nu\left[-\left(w - \frac{\tilde{m}}{2}\right)\tilde{\rho} + \frac{\Psi_0}{2}\tilde{\rho}^2\right] = \text{const}, \qquad (43)$$

where const is the integration constant. Let us assume that waves propagate in the positive direction of the $\tilde{\zeta}$ axis. For the perturbations and their derivatives approaching zero as their coordinates tend to infinity ($\lim_{\tilde{\zeta}\to\infty} \tilde{\rho} = 0$, $\lim_{\tilde{\zeta}\to\infty} \frac{\partial \tilde{\rho}}{\partial \tilde{\zeta}} = 0$, $\lim_{\tilde{\zeta}\to\infty} \frac{\partial^2 \tilde{\rho}}{\partial \tilde{\zeta}^2} = 0$, etc.), the integration constant should be set to zero const $= 0$. By this step, we limit the range of possible solutions and focus only on the structures of interest, i.e., on structures propagating through the unperturbed medium.

Equation (43) belongs to the class of Lienard-type equations [57], which does not have any general analytical solution. However, if we neglect high-frequency dissipative effects (the role of which, in the current research, is played by thermal conduction), i.e., we assume that $\mu_\infty = 0$, it becomes possible to define analytically the discontinuous solutions. Nevertheless, the influence of this coefficient will be taken into account during the numerical solution of Eq. (33) and its analysis on the phase plane (see Sec. VII).

The assumptions mentioned above allow to reduce Eq. (43) into a simpler form:

$$\frac{\partial \tilde{\rho}}{\partial \tilde{\zeta}} = \frac{1}{\sigma} \frac{(\tilde{\rho} - \rho_i)}{(\tilde{\rho} - \rho_a)} \tilde{\rho}, \qquad (44)$$

where

$$\sigma = \frac{2}{\nu} \frac{\Psi_\infty}{\Psi_0}, \qquad \rho_i = \frac{2w - \tilde{m}}{\Psi_0}, \qquad \rho_a = \frac{w}{\Psi_\infty}. \qquad (45)$$

It follows from Eq. (44) that the spatial derivative tends to infinity $\partial \tilde{\rho}/\partial \tilde{\zeta} \to \infty$ when density is equal to ρ_a, which is the turning point of possible integral curves.

In addition, the spatial derivative of density perturbation has two zero (stationary) points $\partial \tilde{\rho}/\partial \tilde{\zeta} = 0$ which are equal to

0 and ρ_i, respectively. It would not be superfluous to mention that the zero point ρ_i can be interpreted as the magnitude of initially induced shock wave $\rho_i = \lim_{\tilde{\zeta}\to-\infty} \tilde{\rho}$.

The parameter σ defines the orientation of integral curves. Assuming σ to be a positively defined $\sigma > 0$, one may obtain a certain family of integration curves. A family of integration curves in the opposite case $\sigma < 0$ can be easily obtained by replacing $\tilde{\zeta}$ to $-\tilde{\zeta}$. It is to be remembered that in the current research, we focus on the evolution of waves in the medium with isochoric and isobaric stability (i.e., $C_{V0} > 0$, $C_{P0} > 0$), which implies condition $\tilde{m} > 0$ for isentropic instability. For simplicity, we also assume that $\Psi_0 > 0$. The latter condition, in particular, directly follows from the assumption of $C_{V0} > 0$, $C_{P0} > 0$ in the media where the heat-loss function (1) is a simple power function of density and temperature (see Sec. VII for details). Thus, further, we will describe the family of integration curves assuming $\sigma > 0$.

Integration of Eq. (44) allows us to write its solutions in the implicit form

$$\tilde{\zeta} = \zeta_0 + \frac{\sigma \rho_a}{\rho_i} \ln|\tilde{\rho}| + \frac{\sigma(\rho_i - \rho_a)}{\rho_i} \ln|\tilde{\rho} - \rho_i|, \qquad (46)$$

where ζ_0 is an arbitrary constant.

Analyzing Eqs. (44)–(46) one may notice that three domains of introduced parameters ($\rho_i > \rho_a$, $\rho_i = \rho_a$, and $\rho_i < \rho_a$) correspond to integral curves I, II, and III, respectively, with qualitatively different forms (see Fig. 4).

Using the obtained integral curves, we consequently may construct the discontinuous solutions corresponding to them. Due to the fact that $\Psi_\infty > 0$, these discontinuities could only be in the form of changing from higher value of $\tilde{\rho}$ to lower (assuming wave propagation direction along the positive direction of the $\tilde{\zeta}$ axis). And as a consequence, the magnitude and speed of initially induced shock wave must be positively defined (i.e., $\rho_i > 0$, $w > 0$).

In order to construct the discontinuous solutions, we have to define the magnitude of the discontinuity (shock jump). To define the magnitude of the shock jump, we should integrate Eq. (43) next to the position of this shock jump $\tilde{\zeta}_d$:

$$(\rho_R - \rho_L)w = \frac{\Psi_\infty}{2}(\rho_R^2 - \rho_L^2),$$
$$\rho_L = \lim_{\tilde{\zeta}\to\tilde{\zeta}_d - 0} \rho,$$
$$\rho_R = \lim_{\tilde{\zeta}\to\tilde{\zeta}_d + 0} \rho.$$

Postulating that on the left side of shock jump the perturbation has density $\rho_L = \rho_d > 0$ and taking into account that on the right side of shock jump $\rho_R = 0$ (up to $\tilde{\zeta} \to \infty$), we can obtain magnitude of the discontinuity (shock jump) as follows:

$$\rho_d = \rho_L = 2\rho_a = \frac{2w}{\Psi_\infty}. \tag{47}$$

Thus, we have three control parameters, namely, the turning point ρ_a, the zero point ρ_i, and the magnitude of the discontinuity ρ_d. A certain relationship between these parameters will determine the shock wave structure corresponding to it. So, we are to define how these parameters may relate to each other.

It follows from Eqs. (45) and (47) that, by the definition $\rho_d > \rho_a > 0$. There is no limitation on zero point ρ_i except its positive sign. Therefore, it may have various positions relative to ρ_d and ρ_a. It is clearly seen from Eqs. (45) and (47), that all control parameters depend on speed w. This suggests that, depending on value w, the relationship between parameters may vary and, consequently, various integral curves and branches of these curves will play a definitive role. Let us introduce two critical values of wave speed w and amplitude of initial perturbation ρ_i (zero point) corresponding to it.

The first critical value corresponds to switching from one branch of integral curve I (Fig. 4) to another and follows from the condition of equivalence between the zero point and the magnitude of the discontinuity ($\rho_i = \rho_d$):

$$w_{cr1} = \frac{\tilde{m}\Psi_\infty}{2(\Psi_\infty - \Psi_0)}, \quad \rho_{cr1} = \frac{\tilde{m}}{\Psi_\infty - \Psi_0}. \tag{48}$$

It can be easily shown that if $\rho_{cr1} > 0$, then the condition $\rho_i > \rho_{cr1}$ means that the solution is defined by the middle branch of integral curve I (Fig. 4), where $\rho_i > \rho_d$. The opposite case $\rho_i < \rho_{cr1}$ means that the solution may be defined by the upper branch of integral curve I or curves II and III, where $\rho_i < \rho_d$.

The second critical value corresponds to switching between the integral curves. This value comes from equivalence between the zero point and the turning point ($\rho_i = \rho_a$):

$$w_{cr2} = \frac{\tilde{m}\Psi_\infty}{2\Psi_\infty - \Psi_0}, \quad \rho_{cr2} = \frac{\tilde{m}}{2\Psi_\infty - \Psi_0}. \tag{49}$$

Similarly, it can be shown that, for the positive value $\rho_{cr2} > 0$, the condition $\rho_i > \rho_{cr2}$ has the meaning for the solution to be defined by integral curve I ($\rho_i > \rho_a$). In the opposite case $\rho_i < \rho_{cr2}$, integral curve III ($\rho_i < \rho_a$) plays its role. The case of equivalence $\rho_i = \rho_{cr2}$ corresponds to integral curve II ($\rho_i = \rho_a$).

However, one may notice that both critical values may become negative due to the low-frequency coefficient of nonlinearity Ψ_0. These conditions are equivalent to impossibility for some relations between control parameters to take place. In particular, in the case of isentropic instability $\tilde{m} > 0$, there is no possibility for inequalities $\rho_i > \rho_d$ and $\rho_i > \rho_a$ to be realized in domains $\Psi_0 > \Psi_\infty$ and $\Psi_0 > 2\Psi_\infty$, respectively.

Now, finally, we may proceed to define and describe the solutions of Eq. (43), which asymptomatically tend to zero points 0 and ρ_i (i.e., $\lim_{\tilde{\zeta} \to \infty} \tilde{\rho} = 0$, $\lim_{\tilde{\zeta} \to -\infty} \tilde{\rho} = \rho_i$). These solutions must be unique and are to include asymptotes, the

section of integral curves, and discontinuities (shock jump). Due to the large amount of introduced parameters and their possible relation between each other, we have decided, for clarity, to show the possible solutions and their implementation conditions in Table I and Fig. 5. The description of these solutions can be found below.

It seems reasonable to begin the description with the structures A–C (Table I) described by *integral curve I*, since they propagate with a greater speed w and require a higher magnitude of initial perturbation ρ_i. Subsequent structures are be ordered, from top to bottom, according to the decreasing value of the wavefront speed w.

(A) The greatest speed w is of *structure A* (see Table I), namely, the shock wave with the smooth density growth behind the front. This type of the solution is realized when the value of the perturbation amplitude ρ_i is more than the value of the shock jump ρ_d ($\rho_i > \rho_d$) which is equivalent to ($\rho_i > \rho_{cr1}$) for $\rho_{cr1} > 0$. The implementation domain for this structure is shown in Table I and Fig. 5. If the necessary condition is fulfilled, then the shock jump ρ_d and shock speed w_d can be found using the following expressions:

$$\rho_d = \frac{\Psi_0\rho_i + \tilde{m}}{\Psi_\infty}, \quad w_d = \frac{\Psi_0\rho_i + \tilde{m}}{2}. \tag{50}$$

(B) In the case when the perturbation amplitude ρ_i is equal to the magnitude of the shock jump ρ_d ($\rho_i = \rho_d$) which is equivalent to ($\rho_i = \rho_{cr1}$) for $\rho_{cr1} > 0$, the solution is a simple step function (see *structure B* in Table I).

(C) The shock wave with the smooth density decrease behind the front (see *structure C* in Table I) is realized when the value of the perturbation amplitude ρ_i is less than the value of shock jump ρ_d and greater than the asymptotic value ρ_a ($\rho_d > \rho_i > \rho_a$) which is equivalent to ($\rho_{cr1} > \rho_i > \rho_{cr2}$) for $\rho_{cr1}, \rho_{cr2} > 0$. The variation of solution realization condition depending on Ψ_0 is shown in Table I. The shock amplitude and speed are defined by expression (50), as well.

(D) The *integral curve II* (see Fig. 4) is realized when $\rho_i = \rho_a \equiv \rho_{cr2}$. This integral curve corresponds to the most interesting structure–the shock pulse (see *structure D* in Table I). This stationary wave has the form of the strongly asymmetric pulse with the sharp front and the long exponential tail:

$$\tilde{\rho}(\zeta) = \begin{cases} \rho_p \exp\left[\frac{(\zeta - \zeta_0)\nu\Psi_0}{2\Psi_\infty}\right], & \zeta \leqslant \zeta_0 \\ 0, & \zeta > \zeta_0 \end{cases}. \tag{51}$$

The amplitude and speed of this pulse are defined by the expressions ρ_p and w_p, respectively:

$$\rho_p = \rho_d = 2\rho_{cr2} = \frac{2\tilde{m}}{(2\Psi_\infty - \Psi_0)},$$

$$w_p = w_{cr2} = \frac{\tilde{m}\Psi_\infty}{(2\Psi_\infty - \Psi_0)}. \tag{52}$$

Here we focus the reader's attention on the fact that the magnitude of this pulse does not depend on the initial perturbation. Thus, this pulse is an autowave (self-sustained) structure. Moreover, as we will show further, such pulses can restore their form upon the interaction with analogous pulses like solitary waves of conservative system. The demonstration of this effect by the numerical modeling can be found in Sec. VII B. It is also essential to note that this solution can

TABLE I. Possible wave structures and their implementation conditions.

Structure	The ratio between the parameters necessary to implement the solution	Condition of the solution implementation in domain $\Psi_\infty > \Psi_0 > 0$, $w_{cr1} > w_{cr2} > 0$	Condition of the solution implementation in domain $\Psi_0 > \Psi_\infty$, $w_{cr2} > 0,\ w_{cr1} < 0$	Condition of the solution implementation in domain $\Psi_0 > 2\Psi_\infty$, $w_{cr2} < w_{cr1} < 0$	The form of possible wave structures
A	$\rho_i > \rho_d > \rho_a$	$\rho_i > \rho_{cr1},\ w > w_{cr1}$	The solution cannot be implemented. In this domain always $\rho_i < \rho_d$. Thus, there is no possibility of switching between branches of integral curve I (Fig. 4).	The solution cannot be implemented. In this domain always $\rho_i < \rho_a$. Thus, there is no possibility for integral curves I and II (Fig. 4) to be realized.	
B	$\rho_i = \rho_d > \rho_a$	$\rho_i = \rho_{cr1},\ w = w_{cr1}$	The solution cannot be implemented. In this domain always $\rho_i < \rho_d$. Thus, there is no possibility of switching between branches of integral curve I (Fig. 4).	The solution cannot be implemented. In this domain always $\rho_i < \rho_a$. Thus, there is no possibility for integral curves I and II (Fig. 4) to be realized.	
C	$\rho_d > \rho_i > \rho_a$	$\rho_{cr1} > \rho_i > \rho_{cr2}$, $w_{cr1} > w > w_{cr2}$	$\rho_i > \rho_{cr2},\ w > w_{cr2}$	The solution cannot be implemented. In this domain always $\rho_i < \rho_a$. Thus, there is no possibility for integral curves I and II (Fig. 4) to be realized.	
D	$\rho_d > \rho_a = \rho_i$	$\rho_i = \rho_{cr2},\ w = w_{cr2}$	$\rho_i = \rho_{cr2},\ w = w_{cr2}$	The solution cannot be implemented. In this domain always $\rho_i < \rho_a$. Thus, there is no possibility for integral curves I and II (Fig. 4) to be realized.	
E	$\rho_d > \rho_a > \rho_i$	$\rho_i < \rho_{cr2},\ w < w_{cr2}$	$\rho_i < \rho_{cr2},\ w < w_{cr2}$	$\rho_i < \infty$	No eligible (single-valued) solutions

exist only in the isentropically unstable medium with the negative dispersion.

Because of all the mentioned properties, the self-sustained shock MA pulses have attracted most of our interest. Therefore, we will give the special attention to this solution.

The described MA pulses have some differences from the analogous solutions for pure acoustic waves described by the NAE. First, the magnitude of fast and slow self-sustained pulses ρ_p has a strong dependence on the direction and strength of the magnetic field. Mainly, due to the dispersion coefficient $\tilde{m}$, which is proportional to the MA increment/decrement $\alpha_{\infty f,s}$ (see Figs. 2 and 3). Second, the fast and slow MA waves cause the distortion of not only pressure and density but also the magnetic field. The nonlinear equation for the perturbation of the magnetic field can be written in analogous way to Eq. (33):

$$\frac{\partial}{\partial \tilde{\xi}}\left(\frac{\partial \tilde{B}_x}{\partial \tilde{\tau}} + \frac{\Psi_{B\infty}}{2}\frac{\partial \tilde{B}_x^2}{\partial \tilde{\xi}} - \mu_\infty \frac{\partial^2 \tilde{B}_x}{\partial \tilde{\xi}^2} \right)$$
$$- \nu\left(\frac{\partial \tilde{B}_x}{\partial \tilde{\tau}} + \frac{\tilde{m}}{2}\frac{\partial \tilde{B}_x}{\partial \tilde{\xi}} + \frac{\Psi_{B0}}{2}\frac{\partial \tilde{B}_x^2}{\partial \tilde{\xi}} \right) = 0, \quad (53)$$

where

$$\Psi_{B\infty} = \frac{\gamma_a \sin\theta}{\gamma_{\infty f,s} - \gamma_\infty}\Psi_\infty, \quad \Psi_{B0} = \frac{\gamma_a \sin\theta}{\gamma_{\infty f,s} - \gamma_\infty}\Psi_0. \quad (54)$$

According to the described solutions, the magnitude of the magnetic field disturbance caused by the self-sustained pulse is defined by the following expression:

$$B_{x,p} = \frac{2\tilde{m}}{2\Psi_{B\infty} - \Psi_{B0}}. \quad (55)$$

Here we should point out the important difference between the density and magnetic field nonlinearity coefficients. For definiteness, let us assume that the density nonlinearity coefficients Ψ_∞ (34) and Ψ_0 (35) for both fast and slow MA waves are positive. Then the coefficients $\Psi_{B\infty}$ and Ψ_{B0} (54) are positive for the fast MA waves, but they change their sign to negative for the slow MA waves. This is due to the fact that the phase velocity of the fast MA waves is always greater than the phase velocity of the acoustic waves $c_{\infty f} \geqslant c_\infty$. Conversely, the phase velocity of the slow MA waves is always lower than the phase velocity of the acoustic waves $c_{\infty s} \leqslant c_\infty$. As a consequence of this changing of the signs, the perturbations
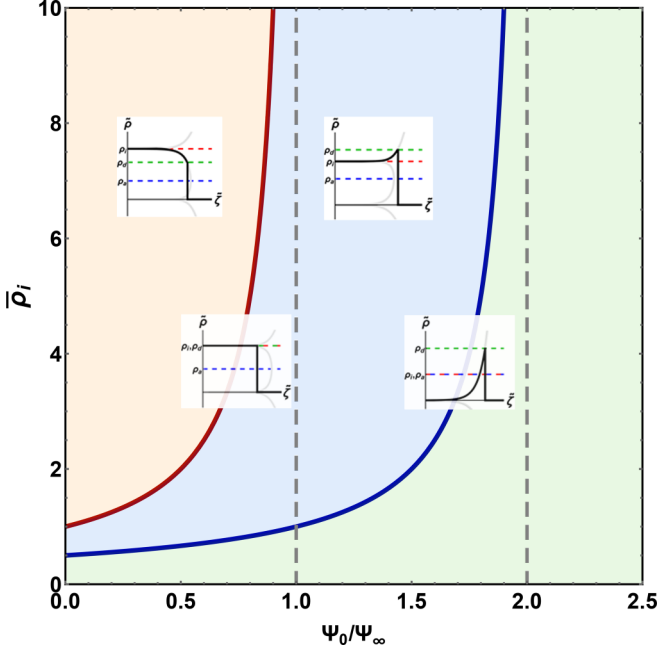
FIG. 5. Bifurcation diagram of Eq. (43). x axis represents the normalized value of Ψ_0. y axis represents the normalized density $\bar{\rho}_i = \rho_i \Psi_\infty / \tilde{m}$. The normalized values of $\bar{\rho}_{cr1} = \rho_{cr1} \Psi_\infty / \tilde{m}$ and $\bar{\rho}_{cr2} = \rho_{cr2} \Psi_\infty / \tilde{m}$ are indicated by red and blue lines, respectively.

of the density and magnetic field are in the same phase in the fast MA wave and are in the opposite phase in the slow MA wave. We will show this feature by the numerical solution of the nonlinear equations for the density and for the magnetic field in Sec. VII.

(E) Finally, we are going to speak about structures coming from *integral curve III* (see Fig. 4). One can easily show that there are *no eligible (single-valued) solutions*, which can be obtained using integral curve III. Nevertheless, the realization domain of this integral curve is considerable. As we mentioned previously, it is realized when $(\rho_i < \rho_a)$ which is equivalent to $(\rho_i < \rho_{cr2})$ for $\rho_{cr2} > 0$. For more information about the realization domain of this integral curve see Table I and Fig. 5.

One may put a question what will happen if we induce the initial perturbation with amplitude belonging to the realization domain of integral curve III. At this stage, we only may propose that in the domain $\Psi_0 < 2\Psi_\infty$, where eligible solutions are to exist in principle (see Fig. 5), the perturbation will tend to transforming itself into the stationary wave structure described by *integral curve II*. This hypothesis will be examined and proven in Sec. VII through numerical simulations of the wave evolution.

In summary, we should mention that existence of the given solutions of NMAE is the necessary condition for the realization of the described shock structures but not the sufficient one. For the certain shock wave profile to be realized, it is also necessary that the corresponding solution to be evolutionary stable. In other words, it is necessary for the shock profile to be stable against the weak nonstationary disturbances. The growth of weak disturbances on the wave profile causes wave destruction and subsequent profile restructuring. Due to this

fact, the analysis of the shock wave structures cannot be confined to the searching of the solution for the stationary problem. This problem is nonstationary and could not be reduced to solving ordinary differential equations. We solve the nonstationary problem of MA wave evolution by numerical modeling, which is described in detail in the following section.

VII. NUMERICAL SIMULATION OF THE EVOLUTION OF MAGNETOACOUSTIC WAVES

First, in this section, we will examine the proposed hypothesis that the induced steplike perturbation will tend to transforming itself into the self-sustained pulse (see structure D in Table I) if magnitude of perturbation satisfies some specific conditions. To be more precise, we will investigate evolution of waves with initial magnitude of perturbation ρ which belongs to domain $\rho_i < \rho_{cr2}$, $\Psi_0 < 2\Psi_\infty$ (see Fig. 4) where there are no eligible solutions according to the stationary solutions analysis. Furthermore, we will analyze the nonstationary evolution of such an initial broadband signal as a Gaussian perturbation. Both issues will be investigated by the numerical solution of obtained NMAE (33) (see Sec. VII A). To show that the NMAE describes the evolution of waves with a sufficiently high accuracy, we will compare results obtained numerically by solving the NMAE and full system of MHD equations (see Sec. VII B). Features specific to MA waves will be shown as well.

Before proceeding to the results of numerical simulations, we should say a few words about the heat-loss function which has been used for our numerical simulations. As the theory of the thermal instabilities was initially built and further developed as a necessary element for understanding the effects in the astrophysical media like the interstellar medium, solar atmosphere, etc., we found it appropriate to use the heat-loss function in the form of simple power functions which are widely used for modeling nonadiabatic processes in these media:

$$L(\rho, T) = c_1 \rho^{a_1} T^{b_1}, \quad H(\rho, T) = c_2 \rho^{a_2} T^{b_2}. \quad (56)$$

The choice of the certain heating and cooling functions for the numerical modeling has been based upon the following principles. First, the cooling function is to correspond to cooling due to optically thin radiation, i.e., $L(\rho, T) \sim \rho T^{b_1}$ in erg g^{-1} s^{-1}. The various parametrization for the cooling function can be found in literature (see, for example, Refs. [58–60]). Second, only the isentropic instability condition is satisfied, as simultaneous satisfaction of several

TABLE II. Parameters of shock self-sustained pulses in the plasma with beta $\beta = 2$ and $\beta = 0.5$ for the wave propagation angle $\theta = \pi/4$.

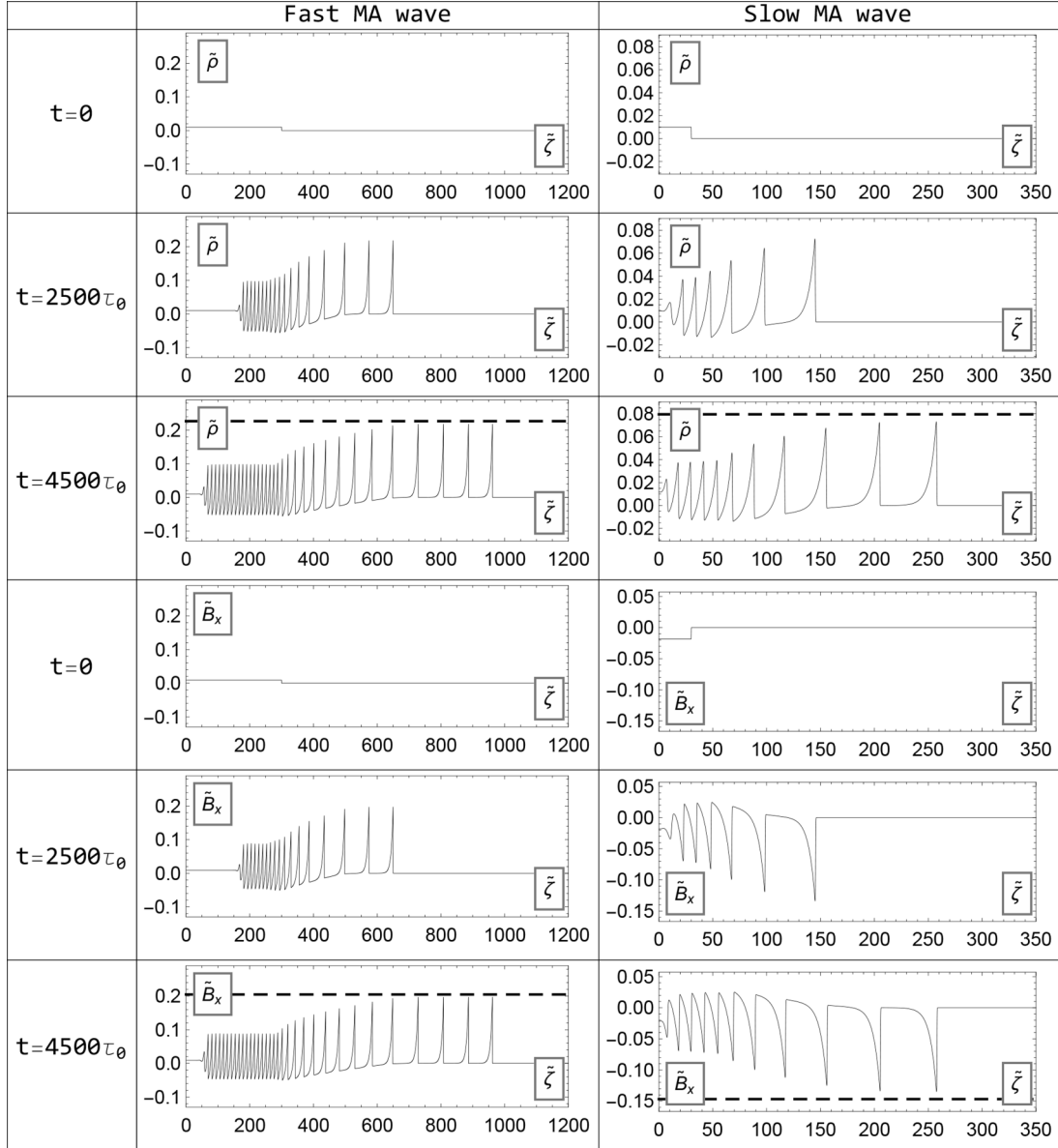|	$\beta = 2$		$\beta = 0.5$	
	Fast wave	Slow wave	Fast wave	Slow wave
ρ_{init}	0.01	0.01	0.01	0.01
ρ_{cr2}	0.113	0.04	0.039	0.116
ρ_p	0.227	0.080	0.078	0.233
$B_{x,p}$	0.205	−0.147	0.092	−0.082

FIG. 6. The decay of fast and slow MA steplike perturbations into a sequence of autowave pulses at $\beta = 2$. Dashed lines correspond to the analytically predicted amplitudes (see Table II). The temporal and spatial steps used in the numerical simulation of the nonlinear equations are $\delta h = \delta \tau = 0.01$. The dimensionless coefficient of the dissipation has been set to $\mu_\infty = 0.005$.

instability conditions puts us beyond the range of applicability of the current analysis. Satisfying these principles, we set the power indices in Eq. (56) equal to $a_1 = 1$, $b_1 = 0.5$, $a_2 = 1.5$, $b_2 = 0.5$. Constants c_1 and c_1 are defined to satisfy $Q(\rho_0, T_0) = 0$.

For the heat-loss function written in the form of simple power functions (56), the low-frequency nonlinearity coefficients can be rewritten in the simpler way:

$$\Psi_{0ac} = \frac{2\gamma_0 - 1}{\gamma_0} + \frac{\gamma_0 - 1}{2}, \tag{57}$$

$$\Psi_0 = \frac{(2\gamma_0 - 1)}{\gamma_{0f,s}} \frac{(\gamma_{0f,s} - \gamma_a \cos^2\theta)}{(2\gamma_{0f,s} - \gamma_a - \gamma_0)} + \frac{3}{2} \frac{(\gamma_{0f,s} - \gamma_0)}{(2\gamma_{0f,s} - \gamma_a - \gamma_0)}$$
$$- \frac{(\gamma_{0f,s} - \gamma_a \cos^2\theta)(2 - \gamma_0)(\gamma_0 - 1)}{2\gamma_{0f,s}(2\gamma_{0f,s} - \gamma_a - \gamma_0)}. \tag{58}$$

Furthermore, it can be shown that if the heat-loss function is written in general form (56) and satisfies the mentioned above principles, then the low-frequency coefficient is always greater than the high-frequency coefficient:

$$\Psi_0 > \Psi_\infty. \tag{59}$$

Thus, a shock wave with a smooth growth behind the front (structure A, see Table I), which is the typical shock wave structure in relaxing media, cannot be realized in media with a given function model (see Fig. 4 and Table I).

A. Numerical simulations of NMAEs: Trains of self-sustained MA pulses

In order to substantiate the predictions of the theoretical model, examine the proposed hypothesis and show the
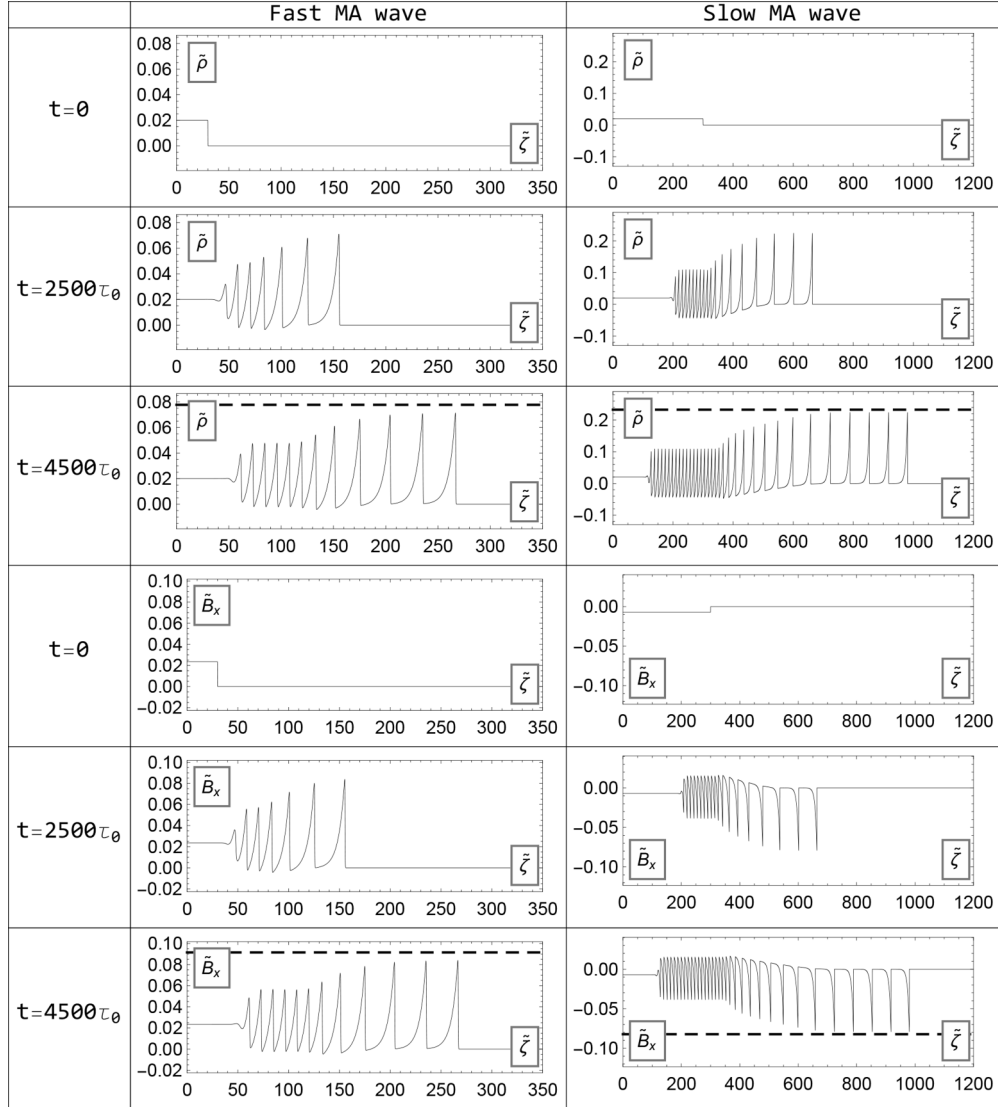
FIG. 7. The decay of fast and slow MA steplike perturbations into a sequence of autowave pulses at $\beta = 0.5$. Dashed lines correspond to the analytically predicted amplitudes (see Table II). The temporal and spatial steps used in the numerical simulation of the nonlinear equations are $\delta h = \delta \tau = 0.01$. The dimensionless coefficient of the dissipation has been set to $\mu_\infty = 0.005$.

evolutionary stability of the described structures, we solve the obtained NMAEs for perturbations of density (33) and magnetic field (53) numerically using the method of splitting [5]. The evolution of fast and slow magnetoacoustic waves is considered separately.

We start with testing the proposed hypothesis and investigating the evolution of initial perturbation in the form of a step function. The initial perturbation of the magnetic field is adjusted in order to correspond to the density perturbation. For definiteness, we assume that the angle between the wave propagation direction and the magnetic field vector is equal to $\theta = \pi/4$. In order to show that in the high-beta plasma the fast MA pulses will reach the greater amplitude than slow MA pulses, we perform the calculation using plasma beta $\beta = 2$. To demonstrate the opposite situation, namely, the stronger amplification of slow MA wave, we use plasma beta $\beta = 0.5$.

Using the above-described parameters of the heat-loss function and wave propagation conditions, one can calculate

the magnitudes of autowave pulses for perturbation of density ρ_p (52) and magnetic field $B_{x,p}$ (55) and define the critical value ρ_{cr2}. These parameters, as well as the amplitude of the initial perturbation in the form of a step function ρ_{init}, are shown in Table II.

In Figs. 6 and 7, one may find results of numerical simulation demonstrating the nonstationary evolution of fast and slow MA steplike perturbations. It is clearly seen that the initial perturbation with amplitude $\rho_{\text{init}} < \rho_{cr2}$ becomes unstable and decays into a sequence of self-sustained shock pulses with amplitudes predicted ρ_p (52) and $B_{x,p}$ (55).

The presented figures show a good agreement between analytically predicted amplitudes and numerical results. The uncertainty in the pulse amplitude is not more than 10% and caused predominately by using the dissipation coefficient. One may notice that the perturbations of density and magnetic field are in the phase in the fast MA wave and in the opposite phase in the slow MA wave. The obtained results
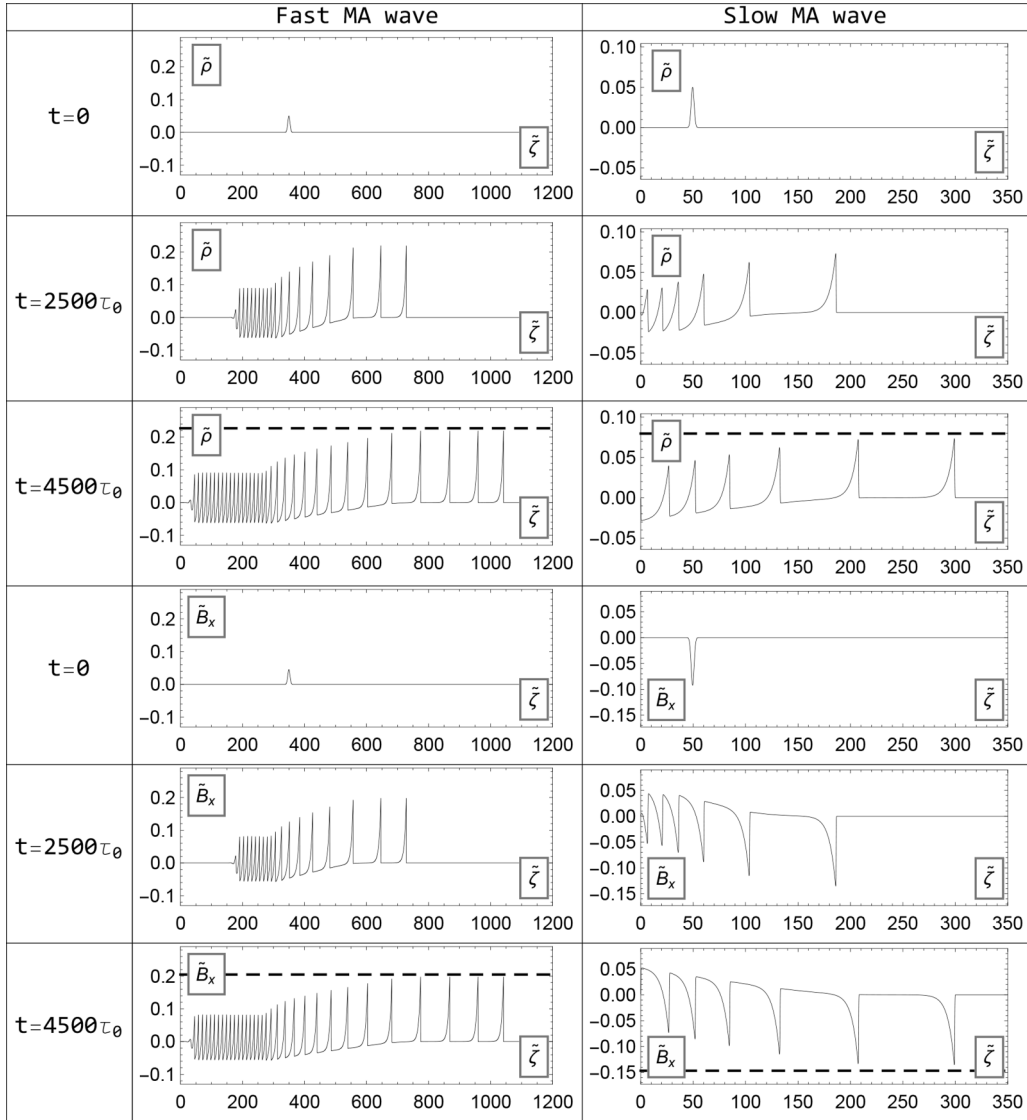
FIG. 8. The decay of a fast and slow magnetogasdynamic wave in the form of Gaussian pulse into a sequence of autowave pulses at $\beta = 2$. Dashed lines correspond to the analytically predicted amplitudes (see Table II). The temporal and spatial steps used in the numerical simulation of the nonlinear equations are $\delta h = \delta \tau = 0.01$. The dimensionless coefficient of the dissipation has been set to $\mu_{\infty} = 0.005$.

also demonstrate the analytically predicted dependences of the amplitudes of shock MA pulses on plasma beta. Namely, fast MA pulses have larger amplitudes than slow MA pulses in the high-beta plasma and *vice versa*.

In order to show that shock pulses will be excited not only by steplike perturbations, but also by a localized perturbation, we investigate numerically the evolution of Gaussian perturbation. For definiteness, we choose plasma beta $\beta = 2$. Figure 8 shows that the initial Gaussian perturbation also decays into a sequence of self-sustained shock pulses with theoretically predicted amplitudes ρ_p (52) and $B_{x,p}$ (55).

Thus, it can be seen that the described shock pulse (see structure D in Table I) fits the definition of the autowave, since it does not depend on the initial perturbation and is determined only by the parameters of the medium and the nonadiabatic processes.

B. Numerical simulations of full system of MHD equations: Shock waves disintegration into trains of autopulses

Nonlinear Eqs. (33) and (53) have been obtained using various assumptions and, as a consequence, they describe not exact, but approximate, solutions of the MHD equations. Therefore, one may ask the question whether these equations are sufficiently accurate to describe the evolution of MHD perturbations. In order to show that they describe wave evolution with a sufficiently high accuracy, we will compare results obtained numerically by solving the NMAE and full system of MHD Eqs. (6).

To analyze the nonstationary evolution of the MA waves, we developed a fully conservative implicit finite-difference scheme approximating the system of Eqs. (6) without taking into account the thermal conduction. Nevertheless, we use the artificial viscosity in our simulations to take into account the effects of dissipation and to smear the shock front. Unlike real

TABLE III. Parameters of shock wave with the smooth density decrease behind the front in the plasma with beta $\beta = 2$.

ρ_{cr2}	ρ_{init}	ρ_d
0.103	0.149	0.255

viscosity, it affects only the thin region of the shock front and does not change the wave structure behind the front. The used artificial viscosity was rather weak (ratio between the artificial and bulk viscosities equals $|\eta/\xi_0| = 0.004$). For simplification of the finite-difference scheme programming, Eqs. (6) have been rewritten in the Lagrangian mass coordinates.

At this point, before proceeding further, it seems reasonable to emphasize that the nonlinear Eqs. (33) and (53) have been obtained under the approximation of independence between fast and slow MA waves. In other words, we have considered these waves separately. However, the disintegration of the initial perturbation implies that the slow MA wave will propagate along the medium perturbed by the fast MA wave. This problem requires a specific consideration and will be described in the future publications. Therefore, in order to compare the results of the numerical solution of the full system of MHD Eqs. (6) with the analytical results obtained on the basis of the NMAE solution, we confine ourselves by the consideration of MA waves propagating across the magnetic field ($\theta = \pi/2$), as in this direction only fast MA waves can propagate.

To carry out the numerical simulation using the NMAE, we use the similar parameters of the numerical scheme (temporal/spatial steps, dimensionless dissipation coefficient, etc.) as in Sec. VII A. For a more complete comparison of the results obtained by the NMAE and full system of MHD Eqs. (6), we also construct solutions of NMAE on the phase plane.

First, let us show that if the amplitude of initial steplike perturbation is greater than the second critical value $\rho_{\mathrm{init}} > \rho_{cr2}$, then it will tend to transform itself to the shock wave with the smooth density decrease behind the front (see structure C in Table I). For definiteness, we consider wave in the plasma with beta $\beta = 2$. Using the parameters of the medium and heat-loss function (56), we can define the critical value ρ_{cr2} and obtain the magnitude of shock jump ρ_d for chosen amplitude of initial steplike perturbation ρ_{init} (see Table III).

Figure 9(a) shows the transformation of initial steplike perturbation to the shock wave with the smooth density decrease behind the front. In Fig. 9(b), one may see the phase portrait of nonlinear Eq. (33) obtained for chosen density ρ_{init}. On the phase plane, the shock wave with the smooth density decrease behind the front [Fig. 9(b) bottom] corresponds to the heteroclinic trajectory connecting the node and saddle stationary points [Fig. 9(b) top]. It is clearly seen that an allowance for the dissipative coefficient μ_∞ causes a slight smoothing of the wave front. In Fig. 9(c) we show results obtained by numerical solution of Eq. 33). As one can see, the results obtained by various ways demonstrate a reasonable agreement.
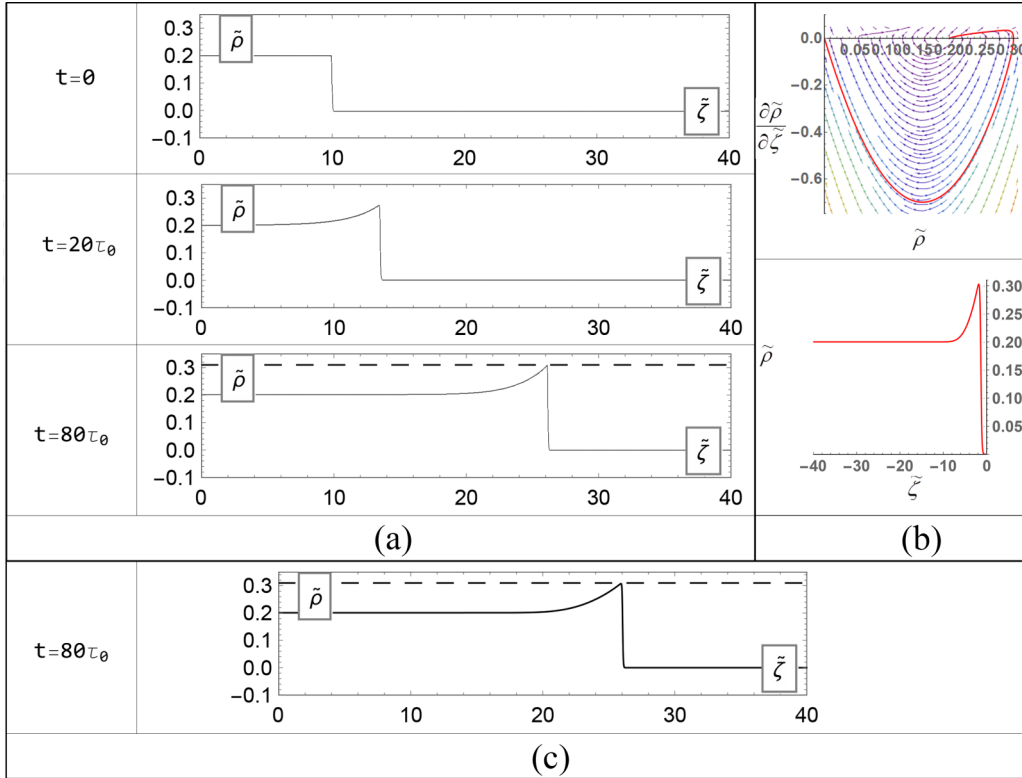

FIG. 9. Formation of the shock wave front with decreasing density behind the front. (a) Numerical simulation of MHD Eqs. (6); (b) (top) phase portrait of stationary nonlinear Eq. (43), (bottom) the stationary structure corresponding to the heteroclinic trajectory connecting the node and saddle stationary points; (c) numerical simulation of the NMAE (33). Dashed lines correspond to the analytically predicted amplitudes (see Table III). The spatial and temporal steps of the grid are $\delta h = 0.0004$ and $\delta t = 0.00025$, respectively.

TABLE IV. Parameters of shock self-sustained pulse in the plasma with beta $\beta = 2$ for the propagation angle $\theta = \pi/2$.

ρ_{cr2}	ρ_{init}	ρ_p
0.103	0.029	0.207

TABLE V. Parameters of shock self-sustained pulse in the plasma with beta $\beta = 1$ for the propagation angle $\theta = \pi/2$.

ρ_{cr2}	ρ_{init}	ρ_p
0.074	0.025	0.148

As we have shown in the Sec. VII A, an induction of the initial steplike perturbation with amplitude less than the second critical value $\rho_{\text{init}} < \rho_{cr2}$ will result in formation of self-sustained pulses (structure D, Table I). Assuming again that wave propagates in the plasma with beta $\beta = 2$, we may predict the amplitude of the shock pulses using relation (52) (see Table IV). Figures 10(a) and 10(c) show the decay of the initial perturbation with amplitude $\rho_{\text{init}} < \rho_{cr2}$ (see Table IV) into the sequence of the self-sustained shock pulses. On the phase plane [see Fig. 10(b)], the self-sustained shock pulse corresponds to the homoclinic trajectory (separatrix loop of the saddle).

Further, we will show that the increase of the magnetic field strength results in the decrease of the pulse magnitude. Assuming that $\beta = 1$, we can recalculate the critical value ρ_{cr1} and pulse magnitude ρ_p (see Table V). In Figs. 11(a) and 11(c), one may see disintegration of the initial perturbation into the sequence of the self-sustained shock pulses with smaller amplitude than at $\beta = 2$. The phase portrait corresponding to the obtained structures is shown in Fig. 11(c).

Based on the comparison made, we conclude that NMAEs describe the evolution of weak shock waves with a sufficiently high accuracy.

As we have mentioned in Sec. VI, the self-sustained pulse can restore its form upon the interaction with similar pulse. In Fig. 12 one can see this feature proven by the numerical simulation of the full system of MHD Eqs. (6). In order to model this interaction, we use pulses which were obtained during the simulation of pulse formation in the plasma $\beta = 2$ [see Fig. 10(a)].

Finally, in Fig. 13 one may see a comparison of the autowave pulse structure predicted by the analytical solution (51) (dashed line) and the structure of this pulse obtained on the basis of the solution of the system of MHD equations (solid line). For comparison, we use the pulse obtained for plasma with beta $\beta = 2$ [see Fig. 10(a)].

VIII. DISCUSSION AND CONCLUSION

In this section, we compare obtained nonlinear Eq. (33) with existing analogues and classical nonlinear equations and
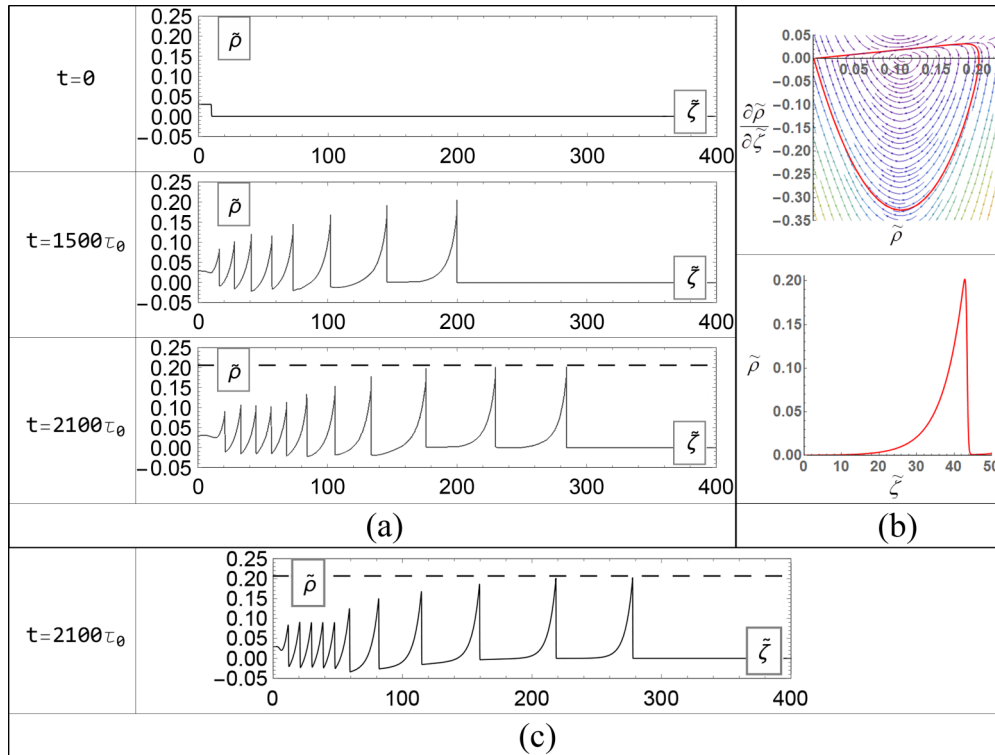

FIG. 10. Decay of the initial perturbation "step" into a sequence of autowave pulses at $\beta = 2$. (a) Numerical simulation of MHD Eqs. (6); (b) (top) phase portrait of stationary nonlinear equation (43), (bottom) the stationary structure corresponding to the homoclinic trajectory (separatrix loop of the saddle); (c) numerical simulation of the NMAE (33). Dashed lines correspond to the analytically predicted amplitudes (see Table IV). The spatial and temporal steps of the grid are $\delta h = 0.0004$ and $\delta t = 0.00025$, respectively.
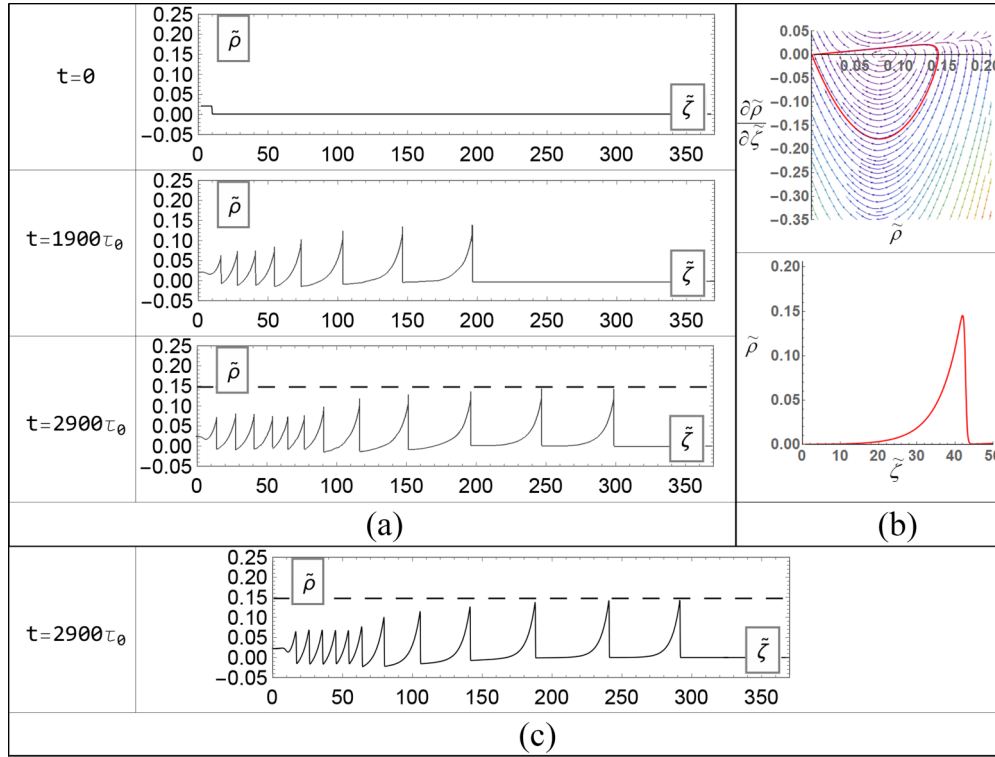
FIG. 11. Decay of the initial perturbation "step" into a sequence of autowave pulses at $\beta = 2$. (a) Numerical simulation of MHD Eqs. (6); (b) (top) phase portrait of stationary nonlinear Eq. (43), (bottom) the stationary structure corresponding to the homoclinic trajectory (separatrix loop of the saddle); (c) numerical simulation of the NMAE (33). Dashed lines correspond to the analytically predicted amplitudes (see Table V). The spatial and temporal steps of the grid are $\delta h = 0.0004$ and $\delta t = 0.00025$, respectively.

explain why this equation is most correctly capable to describe nonlinear waves in the class of media under study.

In order to correctly describe the evolution of a perturbation, nonlinear equations are to take into account all the most significant physical processes, which determine dynamics of perturbation harmonics and interactions between them. First and foremost, such evolutionary equations are to correctly take into account effects manifesting themselves already in a linear approximation.

According to the linear analysis presented in Sec. III, the role of the misbalance between heating and radiation cooling manifests itself in this approximation as several consequences.

The first one is the dispersion of phase velocity of the MA waves (the dependence of phase velocity on frequency).
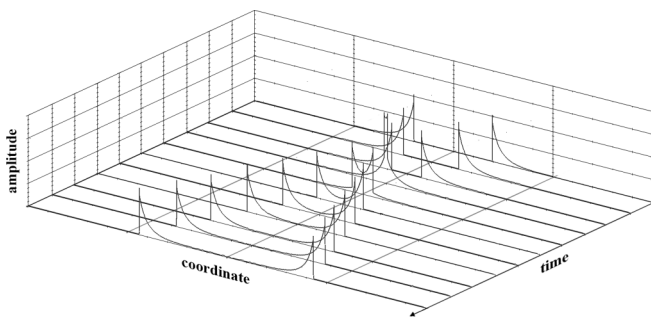

FIG. 12. Restoration of the shape of autowave pulses after the collision.

The next one is an additional dissipation (in the isentropic stability case) or instability/activity of the medium (under conditions of isentropic instability).

And, finally, the increment/decrement characterizing amplification/dissipation of the perturbation also depends on frequency.

It is important to turn our attention to the fact that these effects are caused by only one phenomenon, rather than by several independent phenomena and manifest themselves simultaneously. At the same time, it should bear in mind that
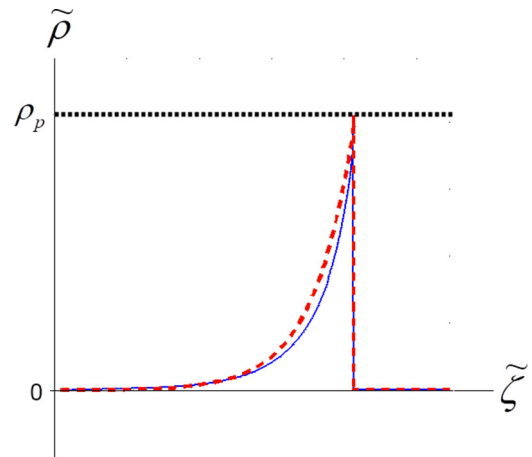

FIG. 13. Comparison of the structure of the shock pulse predicted analytically (dashed red line) and numerically (solid blue line).

in the considered class of media the dissipation processes caused by thermal conductivity, viscosity, finite conductivity, or some other processes play an important role.

Thus, to describe the evolution of waves in a dissipative medium with nonadiabatic processes, the nonlinear equation is to simultaneously take into account dispersion (frequency dependence of phase/group velocity and wave increment/decrement), possible medium activity, and dissipation caused by internal processes in the medium.

For this reason, the Korteweg–de Vries equation

$$a_t + aa_x + \beta a_{xxx} = 0, \qquad (60)$$

which takes into account the dispersion of waves in conservative media, is not applicable for this purpose. The soliton solution of (60) is not the autowave since the amplitude of a soliton depends on the initial perturbation.

For the same reason, the Burgers equation

$$a_t + aa_x - \nu a_{xx} = 0, \qquad (61)$$

which can describe solutions in the form of a shock wave, is not suitable since it only takes into account wave dissipation.

For further descriptions, it would be wise to divide the equations into the ones being "low-frequency" and "high-frequency" analogues of the NAE or NMAE (33) since they can be obtained on their basis by considering the dynamics of waves in the corresponding frequency band and series of additional approximations.

The low-frequency analogues of Eq. (33) are the well-known Korteweg–de Vries-Burgers (KdVB) equations and the modified Kuramoto-Sivashinsky (KS) equation also known as the Kawahara equation [61]. The NAE/NMAE can be reduced to the KdVB and KS equations using the expansion by parameter ϵ ($\omega\tau_0 \sim \epsilon \ll 1$, $\partial\tilde{\rho}/\partial\tilde{\tau} \sim \epsilon\tilde{\rho}$) and taking into account the terms of order ϵ^2 and ϵ^3, respectively [5].

The high-frequency analogues of Eq. (33) are Burgers equation with source term and its various modifications, for example Burgers equation with source and integral dispersion terms, or Burgers equation with nonlinear source term. These equations are also possible to obtain from the NAE/NMAE using expansion by parameter ϵ ($\omega\tau_0 \sim \epsilon^{-1} \gg 1$, $\partial\tilde{\rho}/\partial\tilde{\tau} \sim \epsilon^{-1}\tilde{\rho}$) [5].

Note that all these analogues imply that the phase velocity of perturbation for the whole spectrum is the same, which is incorrect. Therefore, these equations initially do not consider one of the features of new viscosity-dispersion properties determined by nonadiabatic processes. In addition, we should mention that most of analogues take into account only one nonlinearity coefficient.

The KdVB equation which generalizes (60) and (61) has the form

$$a_t + aa_x - \nu_0 a_{xx} + \beta_0 a_{xxx} = 0. \qquad (62)$$

This equation takes into consideration both dissipation and dispersion of waves (positive or negative) and describes more complex nonlinear structures, the so-called dissipative solitons. However, this equation is not capable of taking into account the instability (activity) and dissipation in the medium independently, since everything is described by one term ν_0. Therefore, if the acoustic activity of the medium predominates
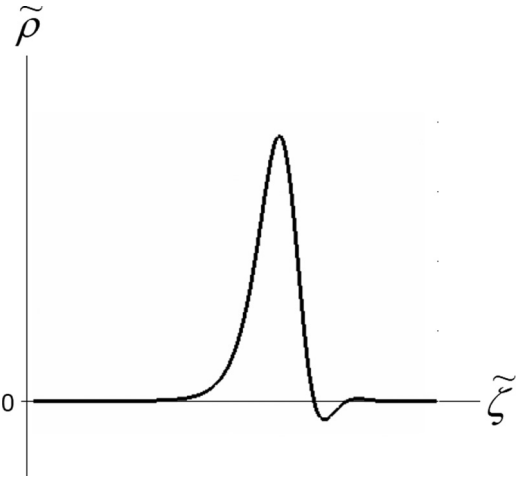

FIG. 14. Qualitative view of the pulse solution predicted by equation 63 in the case of isentropic instability.

over dissipative processes (thermal conductivity, viscosity, etc.), this equation is incapable of describing stationary wave structures. The presence of nonlinear term redistributes energy into high harmonics which, in its turn, will be unlimitedly amplified since dissipative processes are unable to manifest their influence. As noted above, nonlinear Eq. (33) can be reduced to the KdVB type equation with accuracy $\sim\epsilon^2$ if we assume that the perturbation lies only in the low-frequency region of the spectrum with respect to the characteristic heating time ($\omega\tau_0 \ll 1$).

The next example of a nonlinear equation, which can be used to describe the dynamics of waves in an acoustically active medium, is another "low-frequency" analog, namely, the modified KS equation:

$$a_t + aa_x - \nu_0 a_{xx} - \beta_0 a_{xxx} - \eta_0 a_{xxxx} = 0. \qquad (63)$$

In general case, this equation takes into account the activity, dispersion, and dissipation of the medium independently, using coefficients ν_0, β_0, and η_0, respectively. The NMAE (33) can be reduced to Eq. (63) with allowance for higher accuracy orders in the low-frequency approximation [5]. In this case, all the coefficients are proportional to the low-frequency coefficient of bulk viscosity ξ_0 (or in the more general case the sum of the coefficients of viscosity) and do not depend on coefficient μ_∞. Thus, the dissipation of high-frequency harmonics is again not taken into account. At the same time, the presence of a nonlinear term leads to the transfer of energy into high frequencies which do not belong to the region of applicability of this equation. Numerical simulation [47] shows the existence of an autowave solution of this equation (using the coefficients obtained in the expansion in terms of the parameter ϵ) in the form of an impulse with a rarefaction region in front. A qualitative view of this solution is shown in Fig. 14 and, apparently, it is very different from the autowave solution of NAE/NMAE.

Now, we discuss the application validity of the "high-frequency" analogues of nonlinear Eq. (33) to analysis of MHD perturbation evolution in isentropically unstable media. If we assume all harmonics of perturbation to be in the high-frequency part of the spectrum $\omega\tau_0 \gg 1$, then the so-called

Burgers equation with source term (BEwS) can be used to describe the evolution of MA perturbations:

$$a_t + \Psi_\infty a a_x + \nu_\infty a - \eta_\infty a_{xx} = 0. \quad (64)$$

Such an equation has been used in Refs. [18,40] to study the influence of nonadiabatic processes on the evolution of acoustic and magnetoacoustic waves, respectively.

Equations of this type, independently, take into account activity of the medium and dissipative processes using terms with coefficients ν_∞, η_∞, respectively. However, they do not take into consideration the phase velocity dispersion. As it is shown in Ref. [19], BEwS (64) has stationary periodic solutions in the form of sawtooth waves. However, these waves are evolutionary unstable with respect to low-frequency/long-wavelength perturbations. In other words, regardless of the initial periodic perturbation form, wave evolution leads to the establishment of a periodic wave with the maximum possible period at the given boundary conditions.

Further, a higher order of accuracy can be given by the nonlinear Burgers equation with source and integral dispersion terms (BEwSID):

$$a_t + \Psi_\infty a a_x + \nu_\infty a - \eta_\infty a_{xx} + \beta_\infty \int a \, dx = 0. \quad (65)$$

This equation also has a stationary solution in the periodic wave form. This solution is slightly different from the sawtooth wave described by BEwS (64). Nevertheless, with the help of numerical simulation [5,47], it can be shown that, despite the higher order of approximation, BEwSID (65) has the same fundamental drawback as BEwS (64): its stationary solutions are evolutionary unstable with respect to low-frequency/long-wavelength perturbations [19].

Another "high-frequency" analog of Eq. (33) is the generalized nonlinear Burgers-Fisher equation (gBFE):

$$a_t + \Psi_\infty a a_x + \nu_\infty a - \eta_\infty a_{xx} + \Psi a^2 = 0. \quad (66)$$

In particular, such equation has been applied for the analysis of magnetoacoustic waves in heat-releasing plasma [39]. Similar equation was used for describing acoustic waves in nonequilibrium gas [62]. In comparison with (64), this equation takes into account the additional nonlinearity determined by nonadiabatic processes. Equation (66) has a wider class of solutions than "high-frequency" Eqs. (64) and (65) mentioned above. In particular, among its stationary solutions, there is an asymmetric self-sustained solitary pulse. However, the spectrum of this pulse does not fully satisfy the accepted high-frequency approximation and contains harmonics far beyond the adequate description by Eq. (66).

Finally, we are going to explain the importance of incorporation into the nonlinear equation of low-frequency and high-frequency phase velocities (or, equivalently, the low-frequency and high-frequency adiabatic indices) as well as the nonlinearity coefficients. In order to do this, we are to discuss the role of these parameters in the description of shock wave structures. For this purpose, we again turn to the analogy between the heat-releasing medium and the nonequilibrium relaxing gas. According to the theory, the presence of a slow time required to establish thermal equilibrium leads to the fact that the shape of the shock wave is determined by the zones of rapid and slow equilibrium establishment. This means that the structure of the wave front is characterized not only by a single

shock adiabat (as in media with no relaxation processes or heat release), but by two shock adiabats, the so-called equilibrium (low-frequency) and frozen (high-frequency) adiabats [51].

The equilibrium adiabat can be obtained by implying that the gas has a complete equilibrium in the final state. In its turn, the frozen adiabat is obtained by using the assumption that slow relaxation processes do not occur at all. In fact, the frozen adiabat coincides with the shock adiabat for an ordinary shock wave propagating in the medium with adiabatic index γ_∞. The equilibrium adiabat has a much more complicated form, which is determined by slow processes. The form of the equilibrium shock adiabat for the nonequilibrium vibrationally excited gas with the negative bulk viscosity coefficient was obtained for the first time in Refs. [51,52] on the basis of the exact solution corresponding to the system of inviscid one-dimensional gasdynamic equations. Subsequently, the bifurcation diagram was constructed and studied [63]. It depicts the dependence of the shock wave qualitative forms on their velocity and the degree of nonequilibrium. According to the results presented in Refs. [1,52,63], for weak shock waves, the frozen and equilibrium adiabats can be approximated and represented up to the second-order accuracy values in terms of specific volume in forms (67) and (68), respectively:

$$P_L - P_R \approx -\gamma_\infty (V_L - V_R) + \gamma_\infty \Psi_\infty (V_L - V_R)^2, \quad (67)$$

$$P_L - P_R \approx -\gamma_0 (V_L - V_R) + \gamma_0 \Psi_0 (V_L - V_R)^2. \quad (68)$$

Here the indices "R" and "L" for pressure and specific volume correspond to the value before and behind the front of the shock wave, respectively. The analysis performed for the nonequilibrium relaxing gas reveals that expressions for γ_0, γ_∞, Ψ_0, Ψ_∞, obtained by approximating the exact solution of the full system of gasdynamic equations, coincide completely with the expressions obtained in the course of NAE derivation.

It is clearly seen from Eqs. (67) and (68) that coefficients γ_0 and γ_∞ determine the corresponding adiabat slope near the initial point. Coefficients Ψ_0 and Ψ_∞ determine the curvature of the corresponding adiabat near the initial point. Due to the fact that heat-releasing plasma and nonequilibrium relaxing gas have the similar dispersion-viscosity mechanism and the similar nonlinear equation describing evolution of weak perturbations, it is possible to transfer physical meaning of quantities γ_0, γ_∞, Ψ_0, and Ψ_∞ obtained for the relaxing gas to analogous quantities obtained for the heat-releasing plasma.

The solutions obtained on the basis of numerical solutions of the initial MHD system and the analytical solutions of NMAE are in close correspondence with each other. Thus, we can come to the conclusion that equations of form (33) take into account the dispersion properties of waves and nonlinear processes in media under consideration in the most general and correct form, and are directly related to the exact solutions of the initial system of equations.

In conclusion, we briefly discuss the main results described in this article.

First, to perform a linear wave analysis, we have used an approach based on an analogy between nonequilibrium relaxing gas and heat-releasing plasma. In the framework of this approach, the dispersion properties of magnetoacoustic waves have been described. It has been shown that the

nonadiabatic processes connected with misbalance of heating and cooling lead to the dependence of phase velocity and increment/decrement on the perturbation frequency. In this case, the dispersion of the phase velocity can be either positive or negative, and waves can be further damped or amplified.

Second, the properties of waves have been analytically studied as functions of the direction and magnitude of the external magnetic field. It has been shown that amplification of fast MA waves is greater than amplification of slow MA waves in the high-beta plasma. In the low-beta plasma, there occurs the opposite situation.

Third, the nonlinear evolution of magnetoacoustic waves in acoustically active heat-releasing plasma has been analyzed. To describe the wave structure under isentropic instability conditions, we have obtained nonlinear magnetoacoustic Eq. (33), which takes into account the most important features of nonadiabatic processes that effect the formation of stationary wave structures. We have described its analytical solutions in the form of shock waves including an autowave MHD pulse and have investigated the dependence of these waves on the direction and magnitude of the external magnetic field.

Finally, the evolutionary stability of the obtained structures has been confirmed with the help of numerical solutions of the NMAE. The applicability of the equation obtained and the correctness of its solutions have been confirmed by the numerical solution of the initial system of MHD equations. It has been shown that the autowave pulses completely recover their shape after the collision.

We see the most important result of our investigation in the fact that in an isentropically unstable plasma, a single perturbation is able to generate undamped periodic trains of self-sustained shock MHD pulses representing regions of increased density and temperature, as well as increased (in fast MA waves) or lower (in slow MA waves) magnetic field. For weakly nonlinear perturbations this process is described by the NMAE with a sufficiently high accuracy. Furthermore, the opposite situation, namely, nonlinear attenuation of magnetoacoustic waves in heat-releasing plasma can be described using the NMAE as well. The nonlinear equation for MA waves presented in our paper is devoid of most of the shortcomings of its analogs. This equation obtained by our team to our best knowledge has never been obtained by any other authors.

As is shown in a number of papers, there can be a considerable amount of isentropically unstable regions in the interstellar medium, in the solar corona, and planetary atmospheres, including the terrestrial one [64]. Therefore, these results are of interest for studying the nature and properties of multifront shock waves and periodic wave trains in these media. However, the theory presented in this paper and the derived nonlinear equation are useful not only for description of wave processes in nonadiabatic plasma. They are also important for various gaseous media with slow processes of thermal equilibrium establishment which are omnipresent in nature and laboratory experiments. Furthermore, investigation of thermal instabilities even in the linear regime in application to the solar atmosphere is of interest, in particular, for explanation of the observed temperature dependence of adiabatic index [65,66] and observed phase shift between perturbations of different plasma parameters [67,68]. And, last but not least,

they are of great interest for the solving inverse problem, for example, for determining the solar corona heating mechanism by the characteristics of propagating waves.

APPENDIX

The nonlinear evolutionary equation described in Sec. V is obtained from the one-dimensional system of MHD Eqs. (6). We conduct the formulation of this equation by using the perturbation theory and taking into account the terms up to the second order of smallness (i.e., we take into account the terms like $a_2/a_0 \sim \cdots \sim \epsilon^2$). In the course of the derivation, we assume that the dissipation is weak and the corresponding coefficients are the terms of the first order of smallness (i.e., $\kappa_z/\rho_0 T_0 \tau_0 \sim \epsilon$). On this basis, we can rewrite the system of the equations that describes only the terms of the second order of smallness in the following way:

$$\frac{\partial B_{2x}}{\partial t} = -\left(B_{0z}\frac{\partial V_{2x}}{\partial z} - B_{0x}\frac{\partial V_{2z}}{\partial z}\right) = \Theta_1, \qquad (A1)$$

$$\rho_0\frac{\partial V_{2x}}{\partial t} - \frac{B_{0z}}{4\pi}\frac{\partial B_{2x}}{\partial z} = \Theta_2, \qquad (A2)$$

$$\rho_0\frac{\partial V_{2z}}{\partial t} - \left(-\frac{\partial P_2}{\partial z} - \frac{B_{0x}}{4\pi}\frac{\partial B_{2x}}{\partial z}\right) = \Theta_3, \qquad (A3)$$

$$\frac{\partial \rho_2}{\partial t} + \rho\frac{\partial V_{2z}}{\partial z} = \Theta_4, \qquad (A4)$$

$$C_{V\infty}\rho_0\frac{\partial T_2}{\partial t} - \frac{k_B}{m}T_0\frac{\partial \rho_2}{\partial t} - \kappa_z\frac{\partial^2 T_1}{\partial z^2}$$
$$= -\rho_0(Q_{0T}T_2 + Q_{0\rho}\rho_2) + \Theta_5, \qquad (A5)$$

$$P_2 - \frac{k_B(T_0\rho_2 + T_2\rho_0)}{m} = \Theta_6. \qquad (A6)$$

The form of nonlinear terms in the right-hand side of Eqs. (A1)–(A6) can be found as follows:

$$\Theta_1 = -B_{1x}\frac{\partial V_{1z}}{\partial z} - V_{1z}\frac{\partial B_{1x}}{\partial z},$$

$$\Theta_2 = -\left(\rho_1\frac{\partial V_{1x}}{\partial t} + \rho_0 V_{1z}\frac{\partial V_{1x}}{\partial z}\right),$$

$$\Theta_3 = \frac{1}{4\pi\mu}\left(B_{1x}\frac{\partial B_{1x}}{\partial z}\right) - \left(\rho_1\frac{\partial V_{1z}}{\partial t} + \rho_0 V_{1z}\frac{\partial V_{1z}}{\partial z}\right),$$

$$\Theta_4 = -\left(\rho_1\frac{\partial V_{1z}}{\partial z} + V_{1z}\frac{\partial \rho_1}{\partial z}\right),$$

$$\Theta_5 = \Theta_{5\infty} + \Theta_{50},$$

$$\Theta_{5\infty} = -\frac{k_B T_0}{m\rho_0}\rho_1\frac{\partial \rho_1}{\partial t} - C_{V\infty}\rho_0 V_{1z}\frac{\partial T_1}{\partial z}$$
$$+ \frac{k_B}{m}T_1\frac{\partial \rho_1}{\partial t} + \frac{k_B}{m}T_0 V_{1z}\frac{\partial \rho_1}{\partial z},$$

$$\Theta_{50} = -\frac{\rho_0}{2}\left(Q_{0\rho\rho}\rho_1^2 + Q_{0TT}T_1^2 + 2Q_{0\rho T}\rho_1 T_1\right),$$

$$\Theta_6 = \frac{k_B T_1 \rho_1}{m}. \tag{A7}$$

The convenient way to derive the nonlinear equation is considering the perturbation of the magnetic field. A brief description of the main steps is presented below. For convenience, we will replace the notations for the partial differentiation operations by indexes as we have done before.

Differentiating Eq. (A1) with respect to t, and Eq. (A2) with respect to z, we obtain the expression for derivative $V_{2z,zt}$ (A8):

$$B_{0x}V_{2z,zt} = c_{az}^2 B_{2x,zz} - B_{2z,tt} + \left(\Theta_{1,t} + \frac{B_{0z}}{\rho_0}\Theta_{2,z}\right). \tag{A8}$$

Then, we define the second-order time derivative of the density perturbation $\rho_{2,tt}$ by rearranging and combining previous expression (A8) and Eq. (A4):

$$\rho_{2,tt} = -\frac{\rho_0}{B_{0x}}\left(c_{az}^2 B_{2x,zz} - B_{2x,tt}\right)$$
$$+ \left[\Theta_{4,t} - \frac{\rho_0}{B_{0x}}\left(\Theta_{1,t} + \frac{B_{0z}}{\rho_0}\Theta_{2,z}\right)\right]. \tag{A9}$$

The second-order spatial derivative of the pressure perturbation $P_{2,zz}$ can be derived from Eq. (A3) differentiated with respect to z and from Eq. (A4) differentiated with respect to t:

$$P_{2,zz} = \rho_{2,tt} - \frac{B_{0x}}{4\pi}B_{2x,zz} + (\Theta_{3,z} - \Theta_{4,t}). \tag{A10}$$

Expressing the temperature T_2 in terms of the density and pressure perturbations and differentiating it twice with respect to z, we can obtain the following equation using formula (A10):

$$T_{2,zz} = \frac{m}{k_B\rho_0}\left(\rho_{2,tt} - \frac{B_{0x}}{4\pi}B_{2x,zz}\right)$$
$$- \frac{T_0}{\rho_0}\rho_{2,zz} + \frac{m}{k_B\rho_0}(\Theta_{3,z} - \Theta_{4,t} - \Theta_{6,zz}). \tag{A11}$$

After these steps, we can obtain the intermediate form of nonlinear Eq. (33) by the differentiating Eq. (A5) twice with respect to coordinate z and time t and substituting previously derived expressions (A9) and (A11):

$$C_{V\infty}\left(B_{2x,tttt} - (c_\infty^2 + c_a^2)B_{2x,ttzz} + c_\infty^2 c_{az}^2 B_{2x,zzzz}\right.$$
$$- \frac{B_{0x}}{\rho_0}\frac{k_B}{C_{V\infty}m}\kappa_z T_{1,tzzzz} + \Theta_{combo1}$$
$$\left.- c_\infty^2\Theta_{combo2} - \frac{B_{0x}}{\rho_0}\frac{k_B}{C_{V\infty}m}\Theta_{5\infty,tzz}\right)_t$$
$$= -\frac{C_{V0}}{\tau_0}\left[B_{2x,tttt} - (c_0^2 + c_a^2)B_{2x,ttzz} + c_0^2 c_{az}^2 B_{2x,zzzz}\right.$$
$$+ \Theta_{combo1} - c_0^2\Theta_{combo2} - \frac{\tau_0}{C_{V0}}\frac{B_{0x}}{\rho_0}\frac{k_B}{m}\Theta_{50,ttzz}\right], \tag{A12}$$

where

$$\Theta_{combo1} = \left[\frac{B_{0x}}{\rho_0}\Theta_{4,ttt} - \left(\Theta_{1,ttt} + \frac{B_{0z}}{\rho_0}\Theta_{2,ttz}\right)\right]$$
$$+ \frac{B_{0x}}{\rho_0}(\Theta_{3,ttz} - \Theta_{4,ttt} - \Theta_{6,ttzz}),$$

$$\Theta_{combo2} = \left[\frac{B_{0x}}{\rho_0}\Theta_{4,tzz} - \left(\Theta_{1,tzz} + \frac{B_{0z}}{\rho_0}\Theta_{2,zzz}\right)\right].$$

Further, we consider fast and slow MA waves separately. To do this, we choose the systems of the coordinates propagating with fast and slow MA wave velocity, respectively. We also use the method of a slowly varying profile. Thus, the change of coordinates can be written as $\xi = z - c_{f,s}t$, $\tau = \epsilon t$, where $\epsilon \ll 1$. Using the slowly varying profile approach is quite reasonable due to smallness of dissipation and nonlinear terms.

The transformation from old coordinates z, t to new ones ξ, τ can be performed by using these relations:

$$a_{2,z} = a_{2,\xi}, \quad a_{2,t} = -c_{f,s}a_{2,\xi} + a_{1,\tau},$$
$$a_{1,z} = a_{1,\xi}, \quad a_{1,t} = -c_{f,s}a_{1,\xi}. \tag{A13}$$

With the foregoing as a background, the linear relations for the perturbations propagating in the stationary motionless medium are written as follows:

$$B_{1x} = B_0\frac{c_{f,s}^2 \sin\theta}{(c_{f,s}^2 - c_{az}^2)}\frac{\rho_1}{\rho_0},$$
$$V_{1x} = -c_{f,s}\frac{c_a^2 \cos\theta \sin\theta}{(c_{f,s}^2 - c_{az}^2)}\frac{\rho_1}{\rho_0},$$
$$V_{1z} = c_{f,s}^2\frac{\rho_1}{\rho_0}, \quad P_1 = c_{Snd}^2\rho_1,$$
$$T_1 = \frac{m}{k_B}\left(c_{Snd}^2 - c_T^2\right)\frac{\rho_1}{\rho_0}. \tag{A14}$$

Using these relations, one can rewrite nonlinear terms (A7) as functions of density perturbation and its derivatives:

$$\Theta_1 = -\frac{B_0}{\rho_0^2}\frac{c_{f,s}^3 \sin\theta}{(c_{f,s}^2 - c_{az}^2)}\rho_{1,\xi}^2,$$

$$\Theta_2 = 0,$$

$$\Theta_3 = -\frac{1}{4\pi}\frac{1}{2}\left(\frac{B_0}{\rho_0}\right)^2\frac{c_{f,s}^4 \sin^2\theta}{(c_{f,s}^2 - c_{az}^2)^2}\rho_{1,\xi}^2,$$

$$\Theta_4 = -\frac{c_{f,s}}{\rho_0}\rho_{1,\xi}^2$$

$$\Theta_{5\infty} = \frac{c_{f,s}}{\rho}\left[2c_T^2 - c_\infty^2\frac{(c_{Snd}^2 - c_T^2)}{(c_\infty^2 - c_T^2)}\right]\frac{1}{2}\rho_{1,\xi}^2,$$

$$\Theta_{50} = \frac{\rho_0}{2}\left\{Q_{0\rho\rho} + Q_{0TT}\left[\frac{m}{k_B\rho_0}\left(c_{Snd}^2 c_T^2\right)\right]^2\right.$$
$$\left.+ 2Q_{0\rho T}\frac{m}{k_B\rho_0}\left(c_{Snd}^2 - c_T^2\right)\right\}\rho_1^2,$$

$$\Theta_6 = \left(c_{Snd}^2 - c_T^2\right)\frac{1}{\rho_0}\rho_1^2. \tag{A15}$$

Further, we are to transform the perturbation of the second order of smallness and its derivatives in a new coordinate system and again to use linear relations (A14). During the derivation, it is convenient to use the relation, which can be easily obtained from dispersion relation $(c_a^2 + c_{Snd}^2)c_{f,s}^2 -$ $c_{f,s}^4 = c_{az}^2 c_{Snd}^2$. After conducting some cumbersome transformations and taking into account the assumption of the weak dispersion, we obtain that Eq. (A12) for density perturbation $\tilde{\rho} = \rho_1/\rho_0$ takes the form of nonlinear Eq. (33) mentioned above.

[1] V. Makaryan and N. Molevich, Plasma Sources Sci. Technol. **16**, 124 (2007).

[2] R. Galimov, N. E. Molevich, and N. Troshkin, Acta Acust. Acust. **98**, 372 (2012).

[3] E. Kogan and N. Molevich, Sov. Phys. J. **29**, 547 (1986).

[4] V. G. Makaryan and N. E. Molevich, Tech. Phys. **50**, 685 (2005).

[5] V. Makaryan and N. Molevich, Fluid Dyn. **39**, 836 (2004).

[6] N. E. Molevich, Otricatelnaya vtoraya vyazkost v dinamike neravnovesnyh gazovyh sred (Negative second viscosity in the dynamics of nonequilibrium gas media), Doctoral thesis, MEPHI, Moscow (2002) (in Russian).

[7] J. W. S. Rayleigh, *The Theory of Sound* (Macmillan and Co., New York, 1896), Vol. 2.

[8] G. B. Field, Astrophys. J. **142**, 531 (1965).

[9] D. Mihalas, *Stellar Atmospheres* (W. H. Freeman and Co., San Francisco, 1978).

[10] E. N. Parker, Astrophys. J. **117**, 431 (1953).

[11] G. Field, D. Goldsmith, and H. Habing, Astrophys. J. **155**, L149 (1969).

[12] M. G. Wolfire, D. Hollenbach, C. F. McKee, A. Tielens, and E. Bakes, Astrophys. J. **443**, 152 (1995).

[13] M. G. Wolfire, C. F. McKee, D. Hollenbach, and A. G. G. M. Tielens, Astrophys. J. **587**, 278 (2003).

[14] B. V. Somov, N. S. Dzhalilov, and J. Staude, Astron. Lett. **33**, 309 (2007).

[15] N. E. Molevich and A. N. Oraevskii, Zh. Eksp. Teor. Fiz. **94**, 128 (1988) [J. Exp. Theor. Phys. **67**, 504 (1988)].

[16] N. E. Molevich, D. I. Zavershinsky, R. N. Galimov, and V. G. Makaryan, Astrophys. Space Sci. **334**, 35 (2011).

[17] M. Oppenheimer, Astrophys. J. **211**, 400 (1977).

[18] K. V. Krasnobaev and V. Y. Tarev, Sov. Astron. **31**, 635 (1987).

[19] E. Ott, W. M. Manheimer, D. L. Book, and J. P. Boris, Phys. Fluids **16**, 855 (1973).

[20] K. V. Krasnobaev, N. E. Sysoev, and V. Y. Tarev, in *Yadernaya fizika, fizika kosmicheskih izluchenij, astronomiya (Nuclear Physics, Cosmic Radiation Physics, Astronomy)*, edited by A. N. Tihonov and V. A. Sadovnichii (Moscow State University, Moscow, 1994), pp. 222–230 (in Russian).

[21] K. V. Krasnobaev, R. R. Tagirova, S. I. Arafailov, and G. Y. Kotova, Astron. Lett. **42**, 460 (2016).

[22] D. Ryashchikov, N. Molevich, and D. Zavershinskii, Tech. Phys. Lett. **44**, 1163 (2018).

[23] K. Krasnobaev and R. Tagirova, Mon. Not. R. Astron. Soc. **469**, 1403 (2017).

[24] I. De Moortel and V. Nakariakov, Philos. Trans. R. Soc. London A **370**, 3193 (2012).

[25] V. Nakariakov *et al.*, Space Sci. Rev. **200**, 75 (2016).

[26] F. Reale, Living Rev. Solar Phys. **11**, 4 (2014).

[27] M. Ruderman, Sol. Phys. **271**, 41 (2011).

[28] T. Wang, L. Ofman, and J. Davila, Astrophys. J. **696**, 1448 (2009).

[29] I. De Moortel, Space Sci. Rev. **149**, 65 (2009).

[30] T. Wang *et al.*, Astrophys. J. Lett. **574**, L101 (2002).

[31] L. Ofman, V. Nakariakov, and N. Sehgal, Astrophys. J. **533**, 1071 (2000).

[32] C. DeForest and J. Gurman, Astrophys. J. Lett. **501**, L217 (1998).

[33] D. Banerjee and S. Krishna Prasad, in *Low-Frequency Waves in Space Plasmas*, Edited by A. Keiling, D.-H. Lee, and V. Nakariakov, Geophysical Monograph Series, Vol. 216 (Wiley, 2016), pp. 419–430.

[34] D. Banerjee *et al.*, Astron. Astrophys. **380**, L39 (2001).

[35] Z. Svestka, Sol. Phys. **152**, 505 (1994).

[36] O. Terekhov *et al.*, Astron. Lett. **28**, 397 (2002).

[37] W. Tongjiang, L. Ofman, J. M Davila, and Y. Su, Astrophys. J. Lett. **751**, L27 (2012).

[38] P. Simões *et al.*, Astrophys. J. **777**, 152 (2013).

[39] R. Chin, E. Verwichte, G. Rowlands, and V. M. Nakariakov, Phys. Plasmas **17**, 032107 (2010).

[40] A. Kelly and V. M. Nakariakov, in *Proceedings of 'SOHO 13—Waves, Oscillations and Small-Scale Transient Events in the Solar Atmosphere: A Joint View from SOHO and TRACE', 29 September – 3 October 2003, Palma de Mallorca, Balearic Islands, Spain*, edited by H. Lacoste (ESA SP-547, 2004), p. 483.

[41] V. M. Nakariakov, C. A. Mendoza-Briceño, and M. H. Ibanez S, Astrophys. J. **528**, 767 (2000).

[42] S. Ibanez, Proc. Int. Astron. Union **3**, 337 (2007).

[43] M. Ibanez, Phys. Plasmas **11**, 5190 (2004).

[44] S. Ibanez, H. Miguel, T. Escalona, and B. Orlando, Astrophys. J. **415**, 335 (1993).

[45] D. Zavershinskii, D. Kolotkov, V. Nakariakov, N. Molevich, and D. Ryashchikov, Phys. Plasmas **26**, 082113 (2019).

[46] D. Y. Kolotkov, V. M. Nakariakov, and D. I. Zavershinskii, Astron. Astrophys. **628**, A133 (2019).

[47] V. G. Makaryan, Struktura gazodinamicheskih vozmushchenij v stacionarno neravnovesnoj srede s ehksponencialnoj modelyu relaksacii, Ph.D. thesis, Samara University, Samara, Russia (2006) (in Russian).

[48] R. N. Galimov, Teoreticheskoe issledovanie udarnovolnovyh iavtovolnovyh gazodinamicheskih struktur v teplovydelyayushchih stacionarno-neravnovesnyh sredah, Ph.D. thesis, KFU, Kazan, Russia (2012) (in Russian).

[49] S. Ibanez, Astrophys. J. **290**, 33 (1985).

[50] S. Ibanez, Astrophys. J. **396**, 717 (1992).

[51] Y. B. Zel'dovich and Y. P. Raizer, *Physics of Shock Waves and High-Temperature Hydrodynamic Phenomena* (Academic Press, New York, 1966), Vol. 1, p. 944.

[52] L. D. Landau and E. M. Lifshitz, *Fluid Mechanics*, 2nd ed., Course of Theoretical Physics (Butterworth-Heinemann, Oxford, 1987), Vol. 6, p. 539.

[53] E. Priest, *Magnetohydrodynamics of the Sun* (Cambridge University Press, Cambridge, 2014), p. 582.

[54] D. I. Zavershinsky and N. E. Molevich, Tech. Phys. Lett. **39**, 676 (2013).

[55] N. Molevich, D. Ryashchikov, and D. Zavershinskiy, Magnetohydrodynamics **52**, 199 (2016).

[56] V. G. Makaryan, N. E. Molevich, and D. P. Porfiriev, Vestnik Samarskogo gosudarstvennogo universiteta (Bulletin of Samara State University) **72**, 13 (2009) (in Russian).

[57] A. Polyanin and V. Zaitsev, *Handbook of Exact Solutions for Ordinary Differential Equations*, 2nd ed. (CRC Press, Boca Raton, FL, 2003).

[58] R. Soler, J. L. Ballester, and S. Parenti, Astron. Astrophys. **540**, A7 (2012).

[59] J. Klimchuk and P. Cargill, Astrophys. J. **553**, 440 (2001).

[60] R. Rosner, W. H. Tucker, and G. S. Vaiana, Astrophys. J. **220**, 643 (1978).

[61] T. Kawahara, Phys. Rev. Lett. **51**, 381 (1983).

[62] I. P. Zavershinskii, E. Kogan, and N. E. Molevich, Izvestiya vuzov. Prikladnaya nelinejnaya dinamika (Izvestiya VUZ. Applied Nonlinear Dynamics) **1**, 87 (1993) (in Russian).

[63] R. Galimov and N. E. Molevich, Fluid Dyn. **44**, 158 (2009).

[64] I. E. Suleimenov, V. M. Aushev, E. A. Tulebekov, and I. A. Antoshchuk, Geomagn. Aeron. **46**, 378 (2006).

[65] T. Van Doorsselaere, N. Wardle, G. Del Zanna, K. Jansari, E. Verwichte, and V. M. Nakariakov, Astrophys. J. Lett. **727**, L32 (2011).

[66] S. K. Prasad, D. B. Jess, and T. Van Doorsselaere, arXiv:1908.00384.

[67] T. Wang, L. Ofman, X. Sun, E. Provornikova, and J. M. Davila, Astrophys. J. Lett. **811**, L13 (2015).

[68] E. G. Kupriyanova, L. K. Kashapova, T. Van Doorsselaere, P. Chowdhury, A. K. Srivastava, and Y.-J. Moon, Mon. Not. R. Astron. Soc. **483**, 5499 (2018).